

The 10<sup>th</sup> Session of East Asia winter Climate Outlook Forum (EASCOF-X)  
10 November 2022, Ulaanbaatar, Mongolia (Online)

# Characteristics of 2022 summer in Japan

NAKAMURA Tetsu,  
Tokyo Climate Center, Japan Meteorological Agency

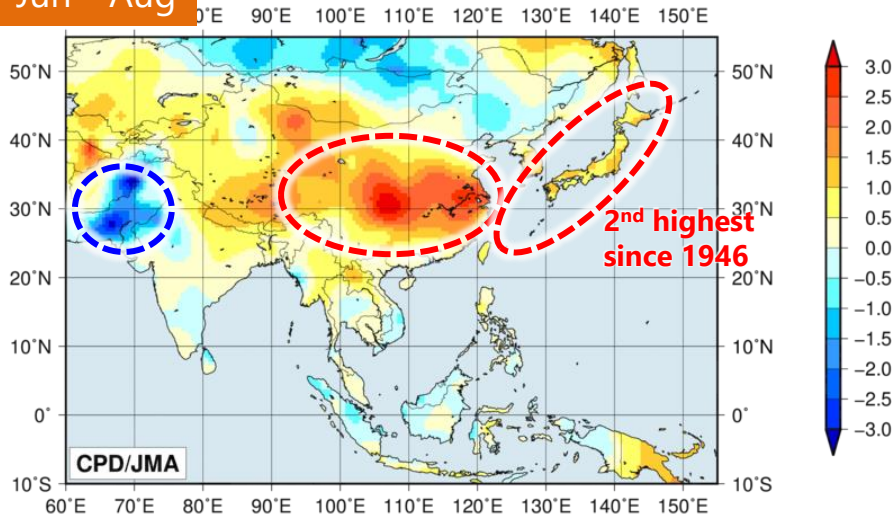
- I. Record-high temperature in late June to early July in Japan
- II. Heavy rain events in mid-July to early August in Japan
  - Partly based on the discussion by the JMA Advisory Panel on Extreme Climate Events\*
  - See also the TCC/JMA's press release about this event  
[https://www.data.jma.go.jp/tcc/tcc/news/press\\_20220914.pdf](https://www.data.jma.go.jp/tcc/tcc/news/press_20220914.pdf)
- III. Summary

\*The JMA Advisory Panel on Extreme Climate Events, consisting of prominent experts on climate science from universities and research institutes, was established in June 2007 by JMA to investigate extreme climate events based on up-to-date information and findings. The current chair is Prof. Hisashi Nakamura from the University of Tokyo.

# 2022 Summer in East Asia

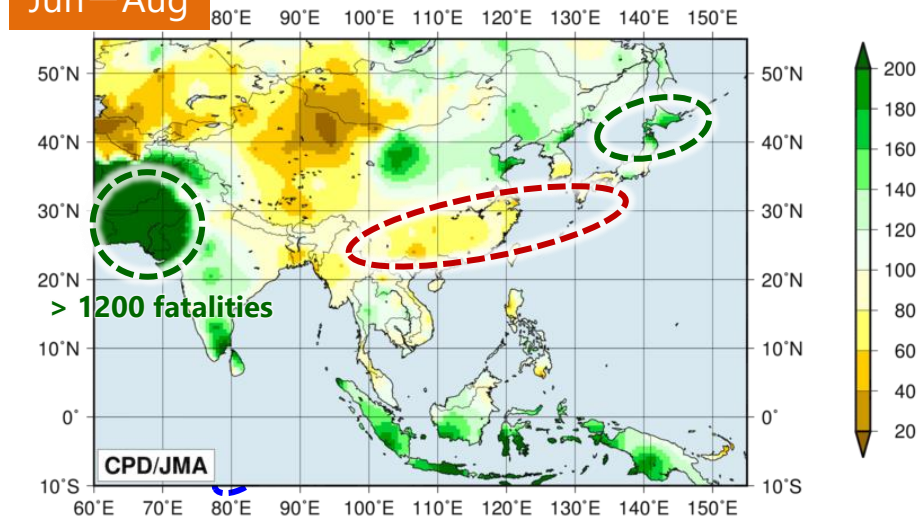
## Temperature Anomaly [°C]

Jun—Aug



## Precipitation Ratio [%]

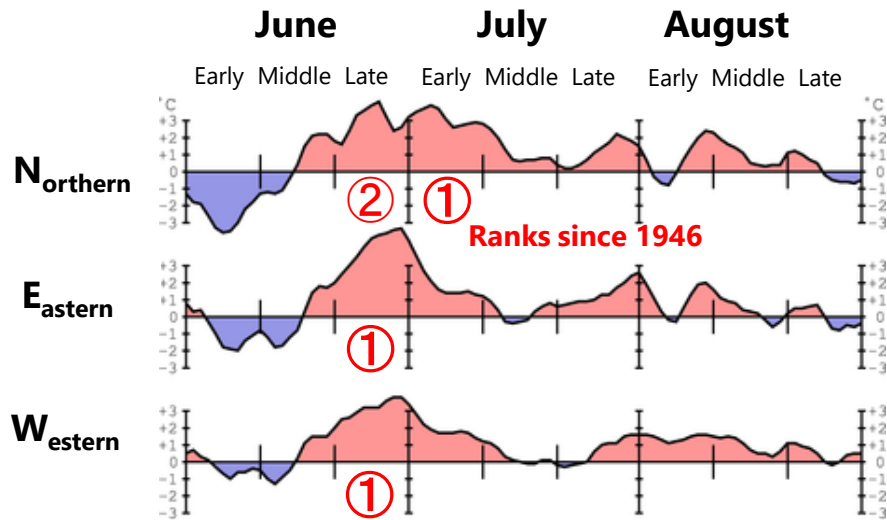
Jun—Aug



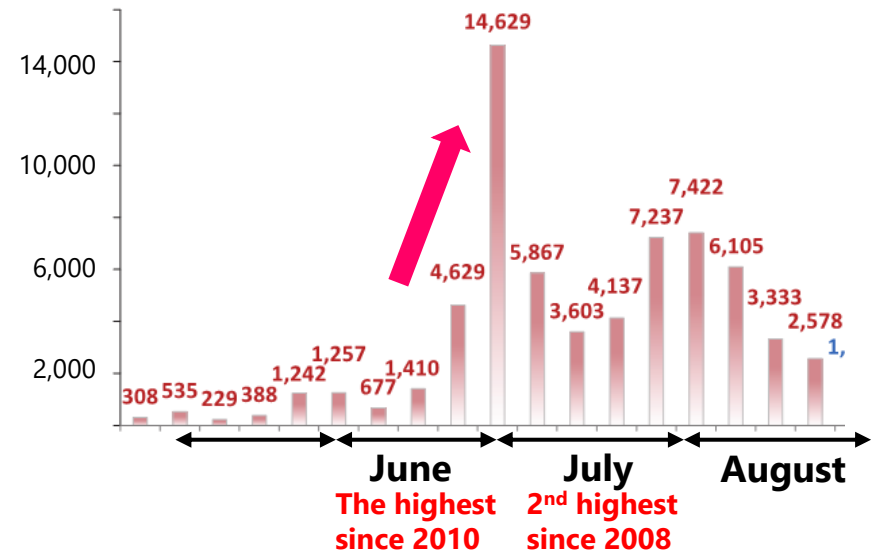
Based on CLIMAT reports. The baseline period for climatological normal is 1991-2020.

- **Over Asia:**
  - Extreme heavy rain in Pakistan
  - Heatwave and drought in China
- **In Japan:**
  - Large fluctuation in a season
    - Record-**high temperature** in late June to early July
    - **Heavy rain** events in July and early August

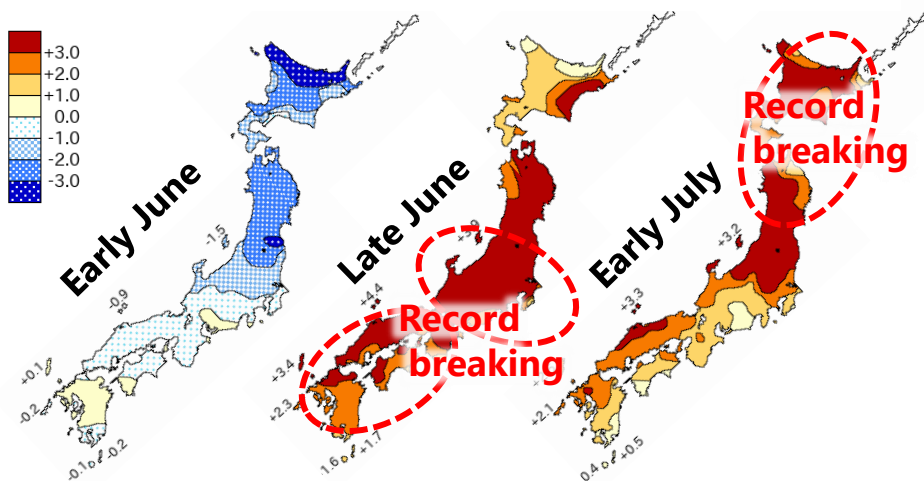
# Record-high temperature



5-day running mean temperature anomalies



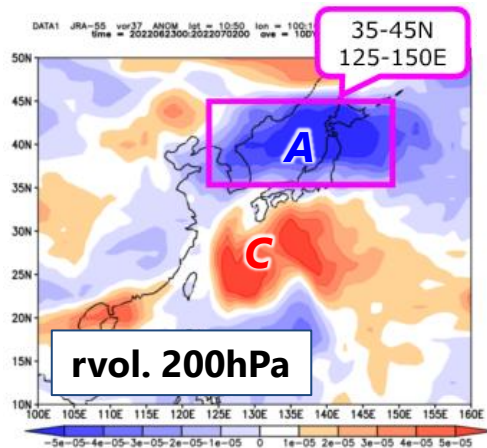
Weekly # of emergency transport due to heatstroke



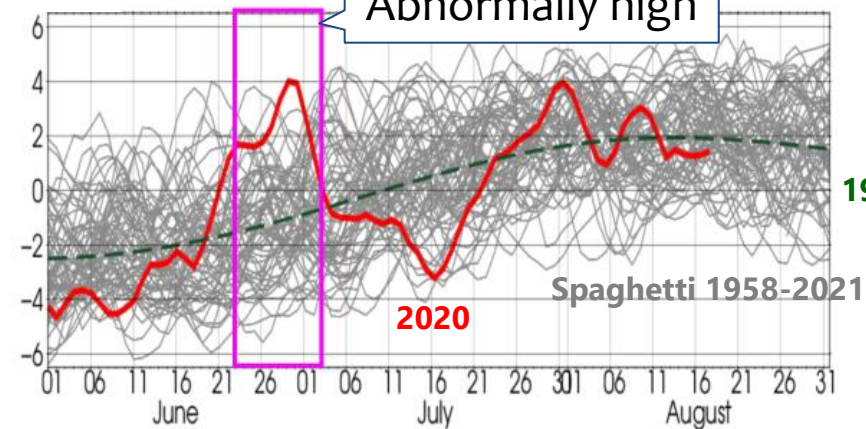
- Record breaking high temperature was observed over Japan in late June to early July.
- Rapid warming caused the record number of heatstroke patients in June.

# Double-High systems

Upper Trop.



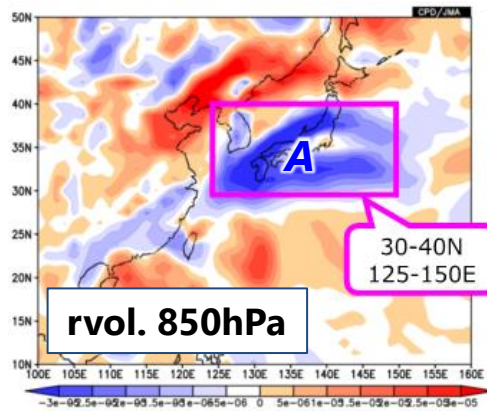
Intensity of  $A_{\text{anti-Cyclone}}$   
( $-10^{-4}/\text{s}$ )



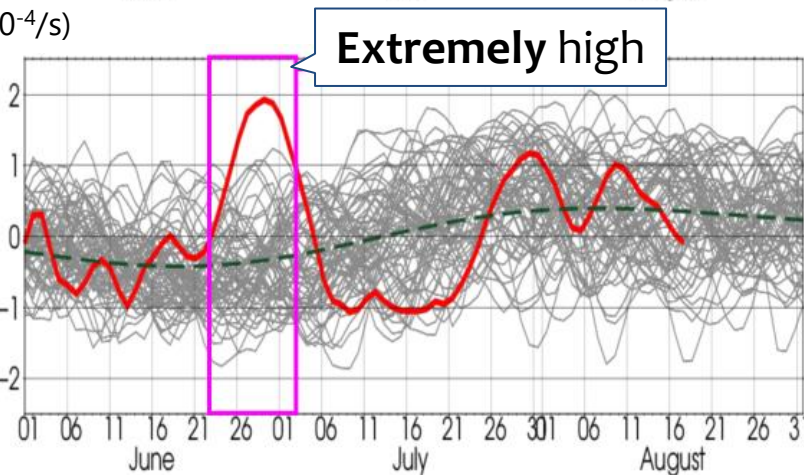
Normal  
1991-2020

Spaghetti 1958-2021

Lower Trop.



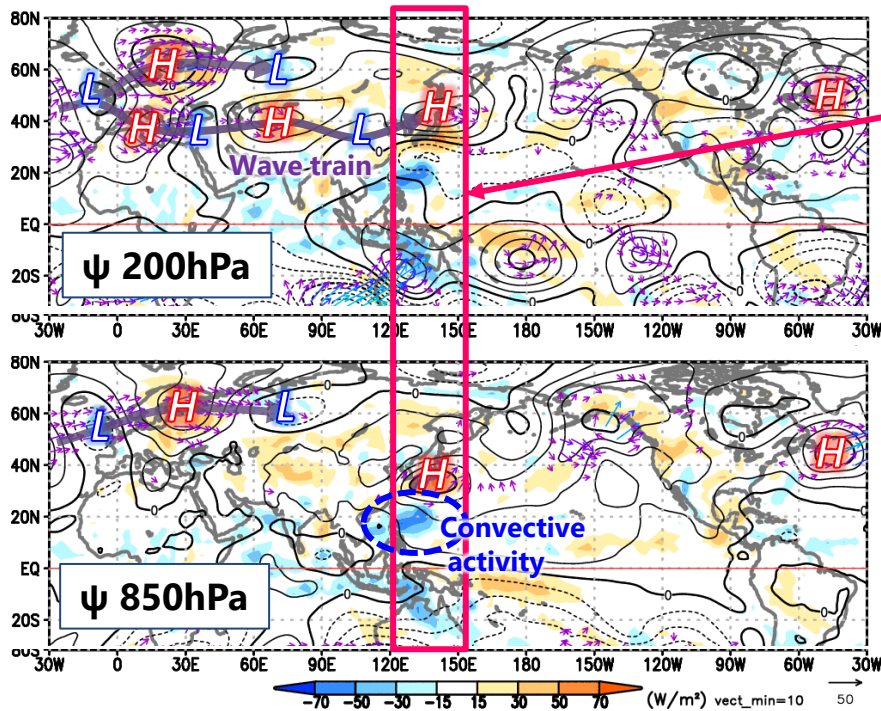
( $-10^{-4}/\text{s}$ )



Rapid development of the **double-High systems** (Imada et al., 2019, SOLA) caused high temperature anomalies over Japan.

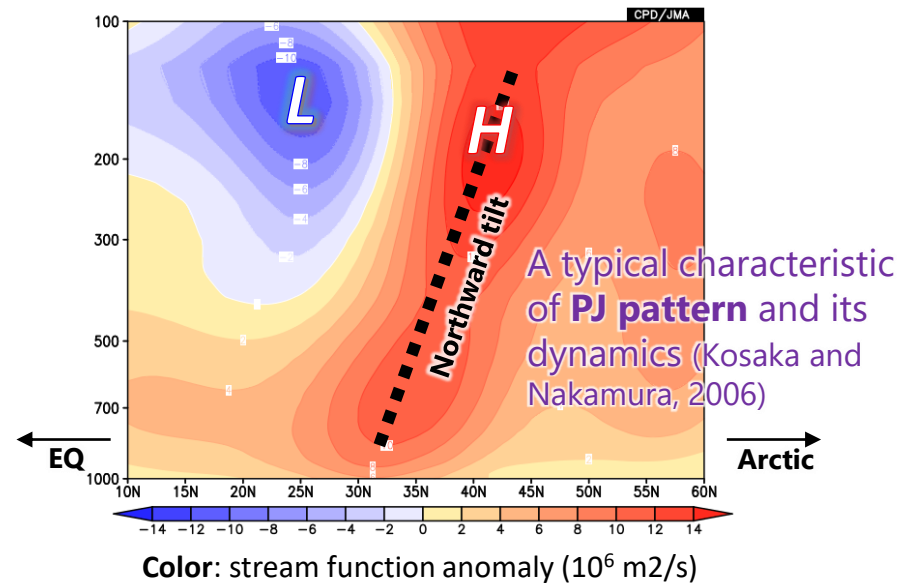
# Silk-Road & PJ pattern

Avg. 23 June-02 July (peak period of event)



Contour: stream function anomaly  
 Arrow: wave activity flux ※Takaya and Nakamura (2001)  
 Shade: OLR anomaly

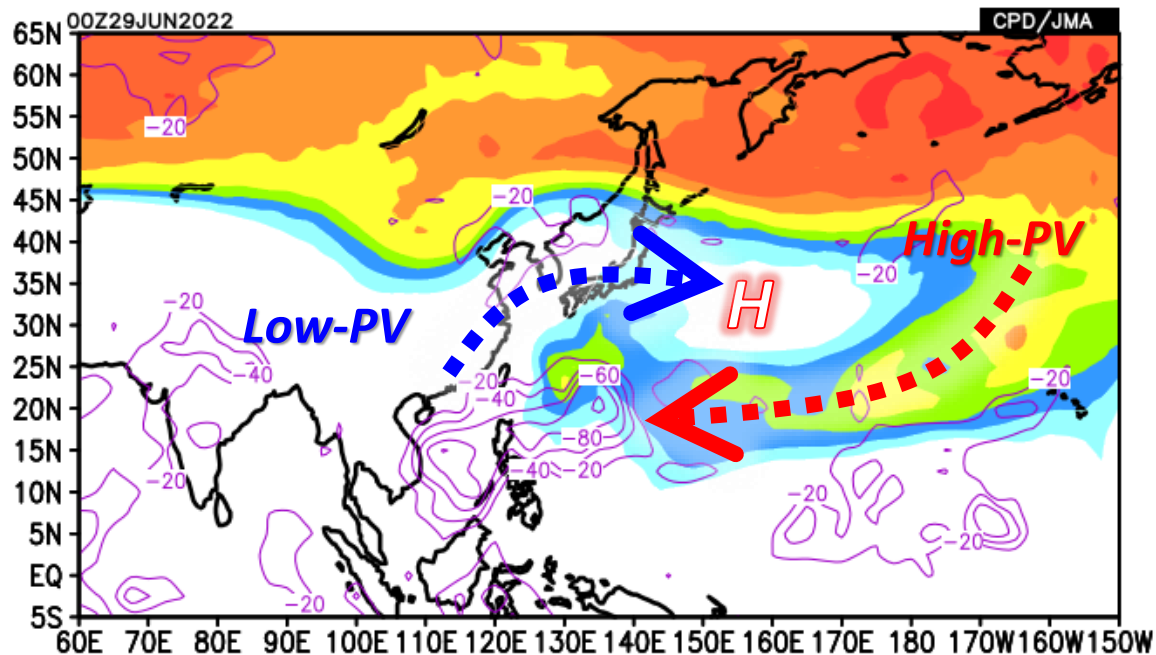
120-150E cross section



Double-high system is possibly induced and maintained by

- Wave train across Eurasia (**Silk-Road pattern**)
- Convective activity around the Philippines (Pacific-Japan/**PJ(-like) pattern**)

Avg. 27.Jun-01.Jul (focused period)



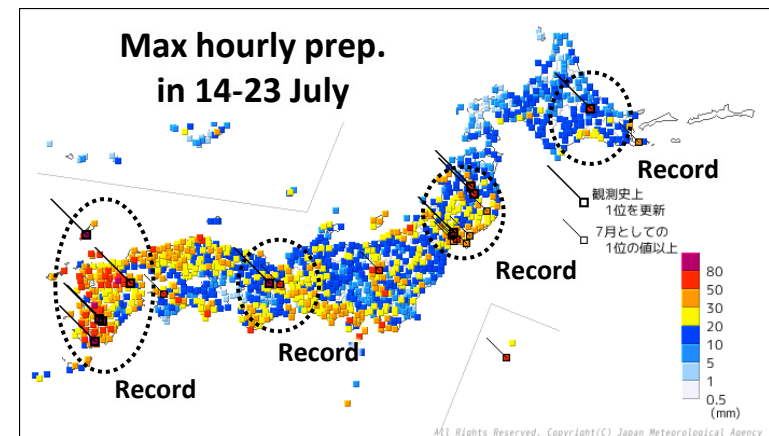
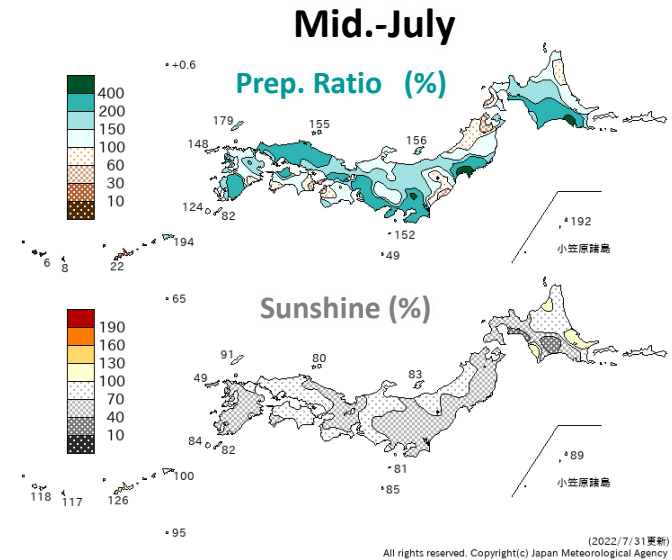
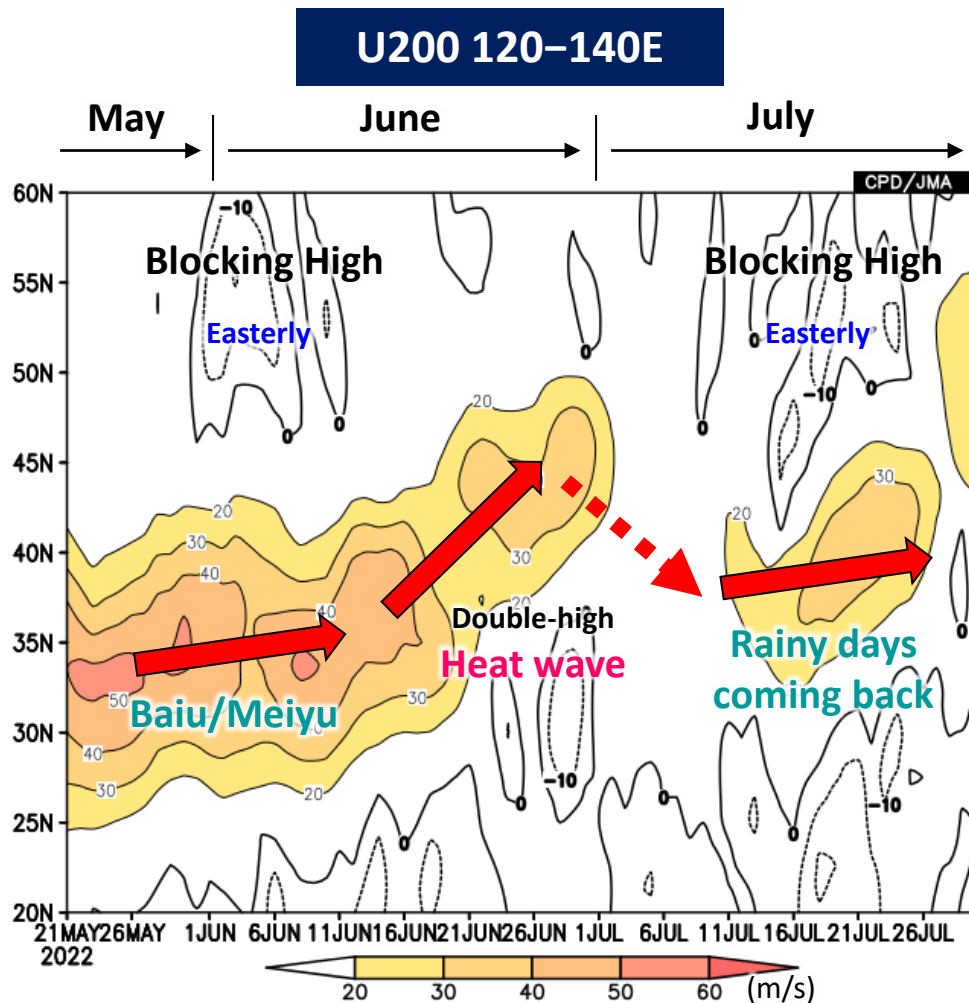
color: PV at 360K surface (PVU)

contour: OLR negative anomaly ( $W/m^2$ )



- Subtropical intrusion of high-PV due to Anti-cyclonic wave breaking
  - > may enhance the convective activity and thus PJ-like pattern
  - > such feedback possibly maintains double-High system

# Rainy days in July



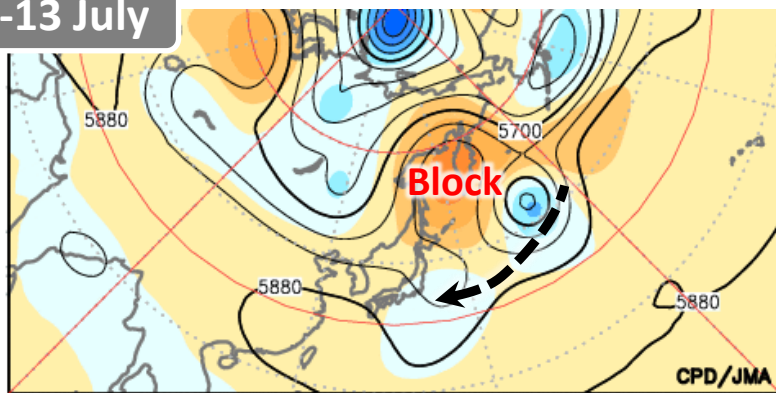
After hot events in late June, rainy and cloudy days came back, due partly to development of **the blocking-high** north of Japan.



# Blocking and high-PV intrusion

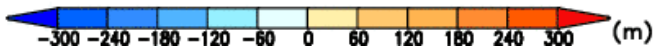
**Z500**

7-13 July



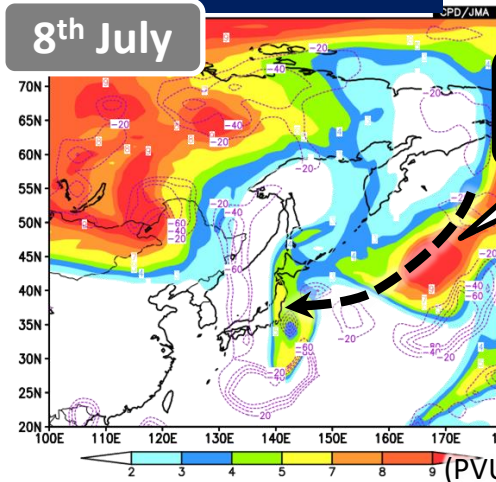
Color: anom

Contour: actual



**PV@350K**

8th July



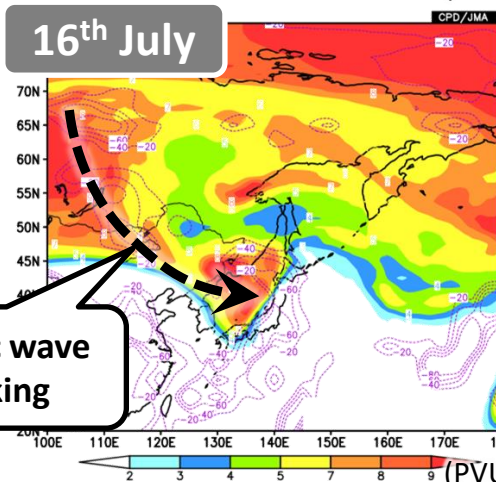
Anti-cyclonic wave braking

Color: 350K PV

Contour:

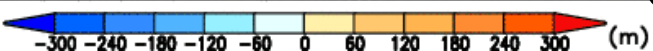
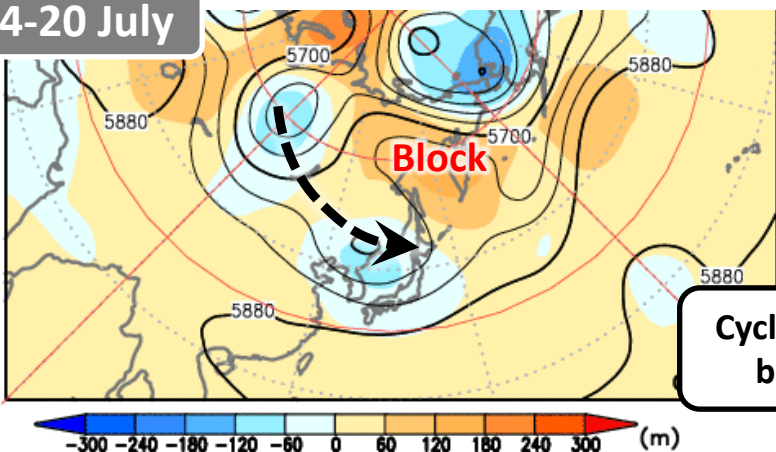
OLR anom ( $W/m^2$ )

16th July



Cyclonic wave breaking

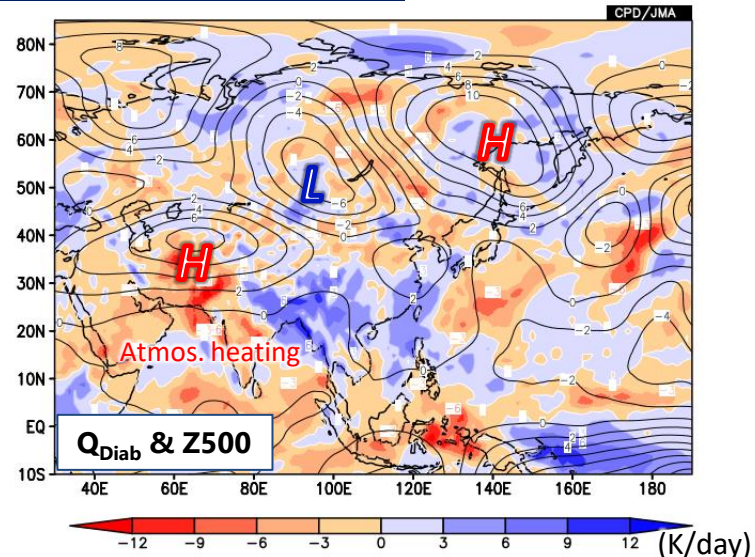
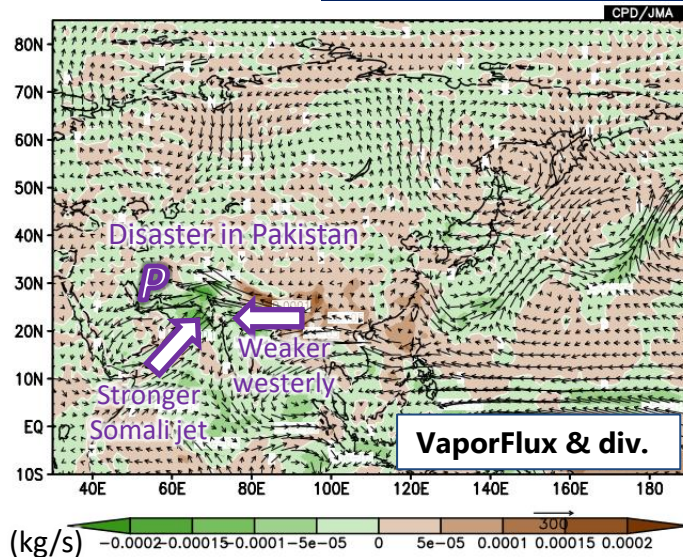
14-20 July



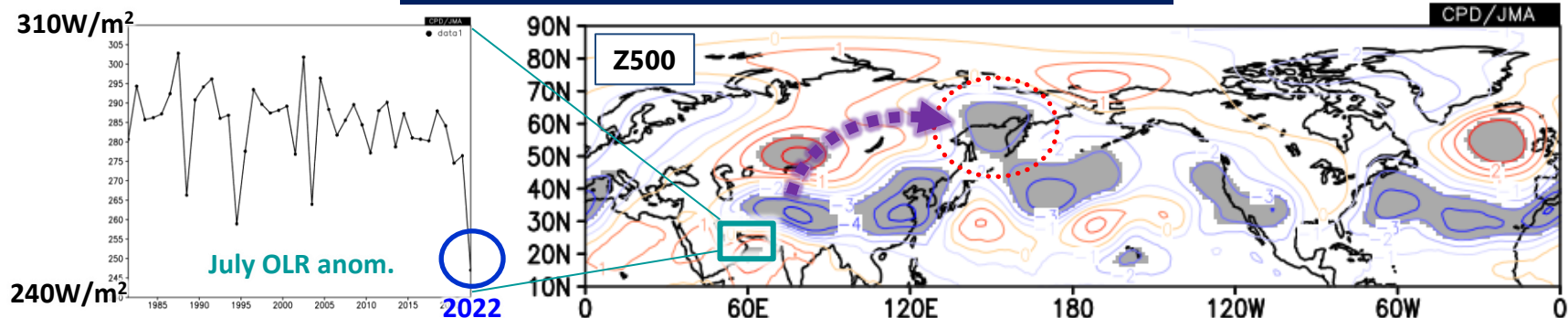
Wave train induced/maintained the blocking over Sea of Okhotsk.  
High-PV intrusion may induce strong rain events broad Japan.

# In relation to Pakistan disaster

## Monthly mean anomalies in July 2022



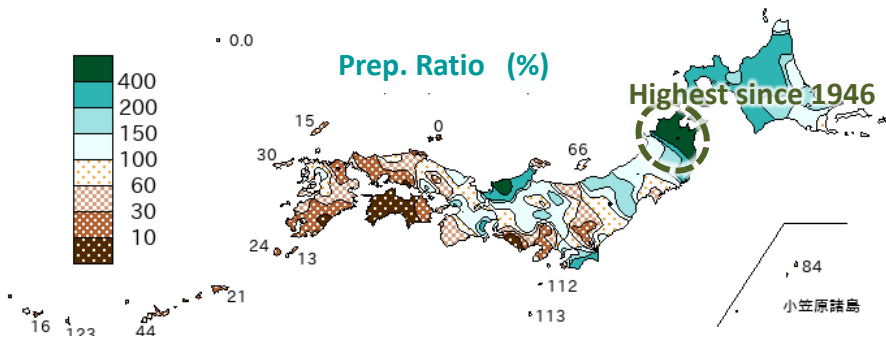
## Regressions onto OLR (50-65E, 20-30N)



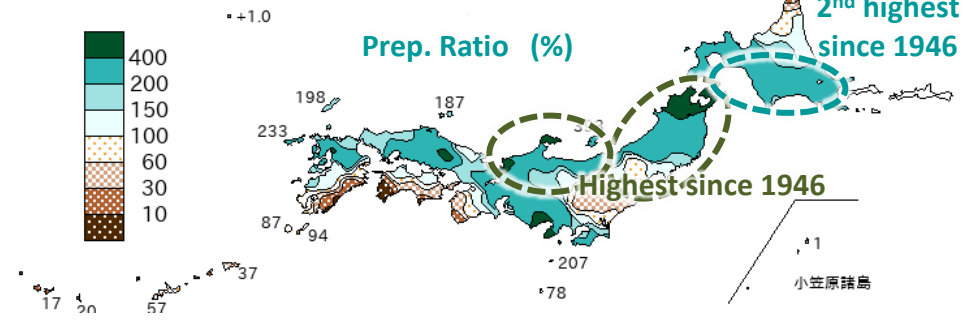
The strongest convection over Pakistan may enhance the Far East blocking as a background forcing. (interaction with Arctic pathway was also suggested)

# August rainfall in northern Japan

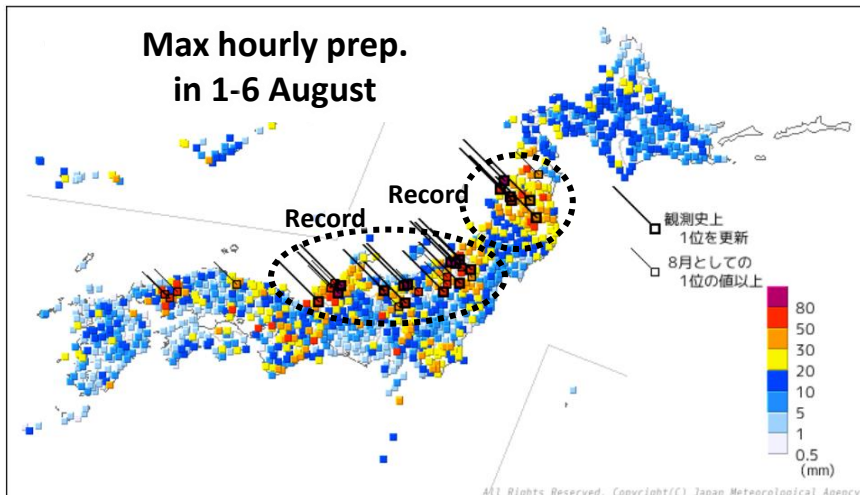
### Early August



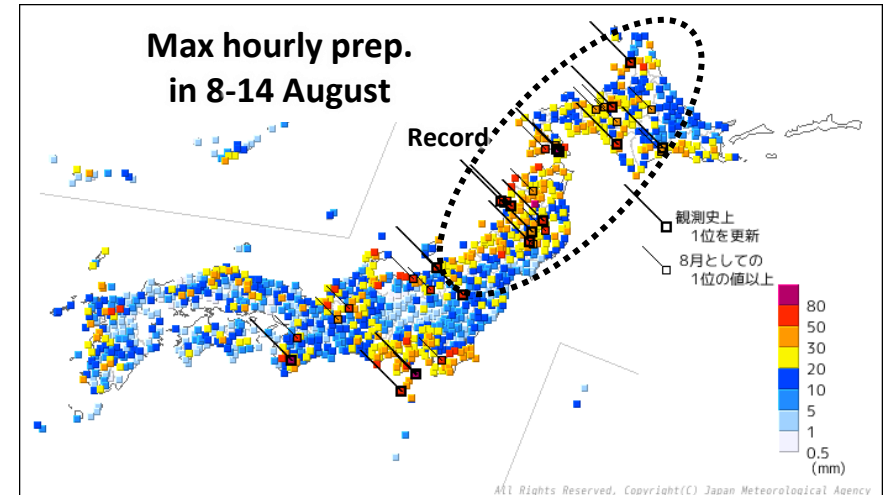
### Mid. August



### Max hourly prep. in 1-6 August

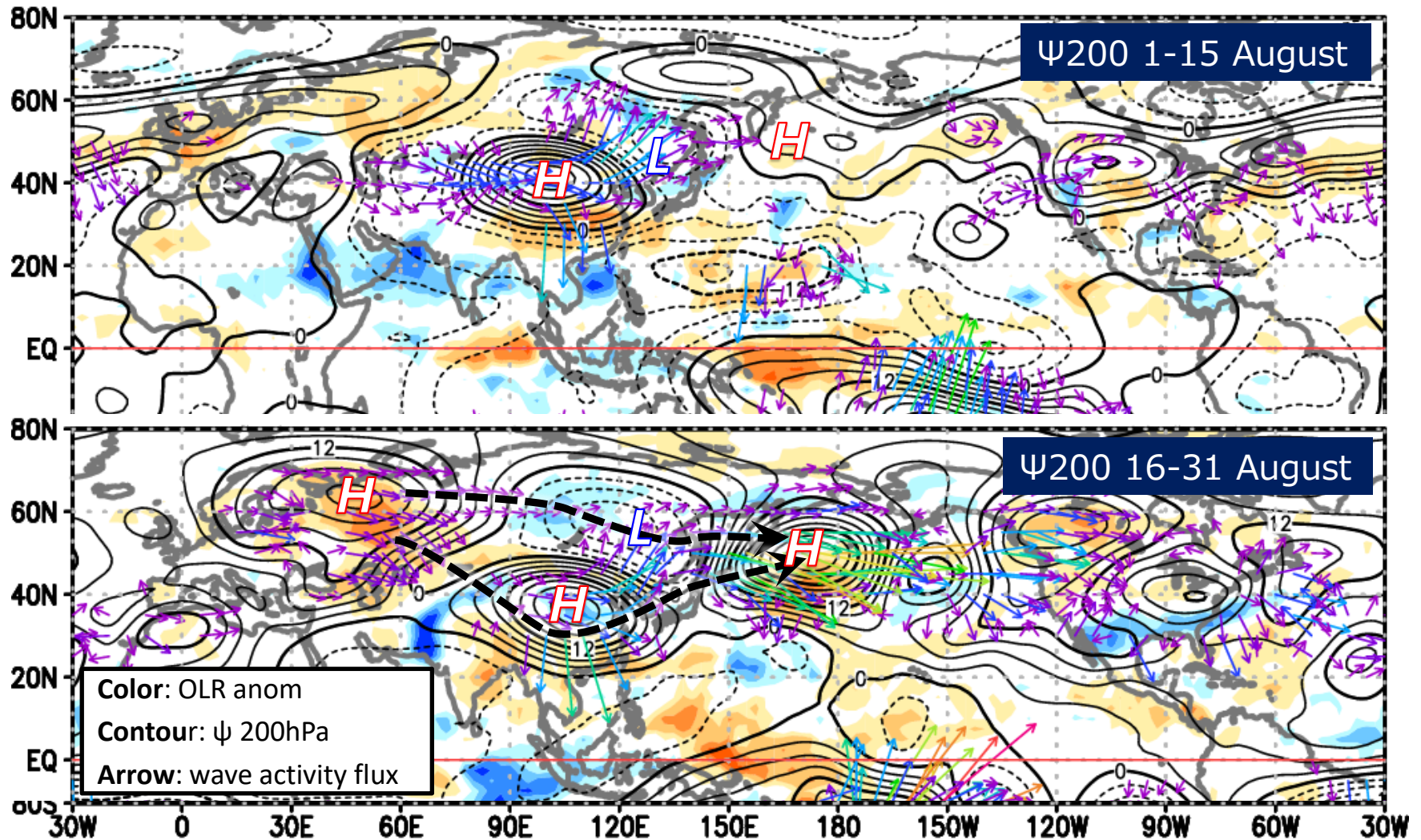


### Max hourly prep. in 8-14 August



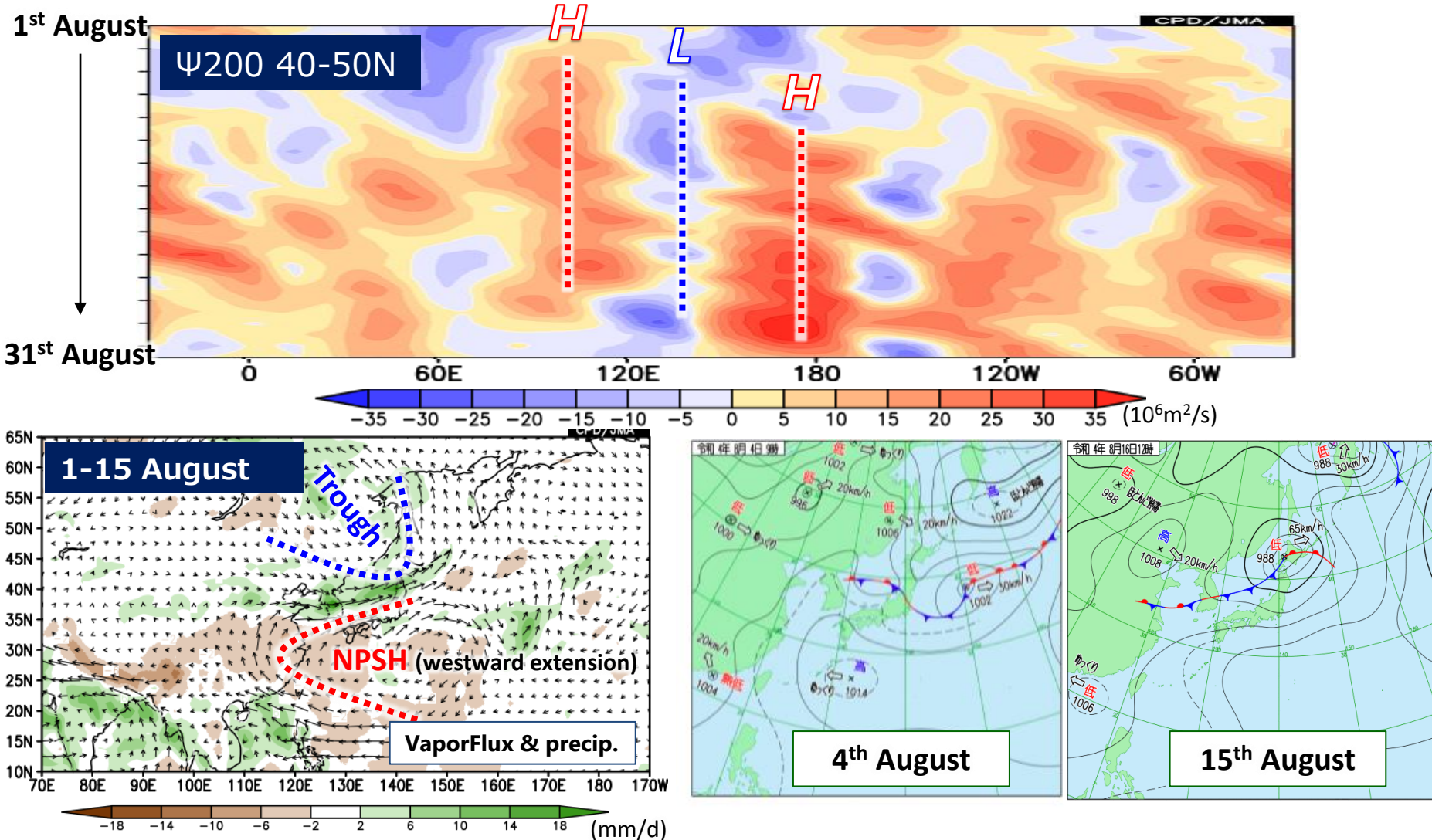
In early to mid- August, heavy rains were observed in northern Japan. River floods caused severe socioeconomic damages in Tohoku region.

# Large-scale circulation



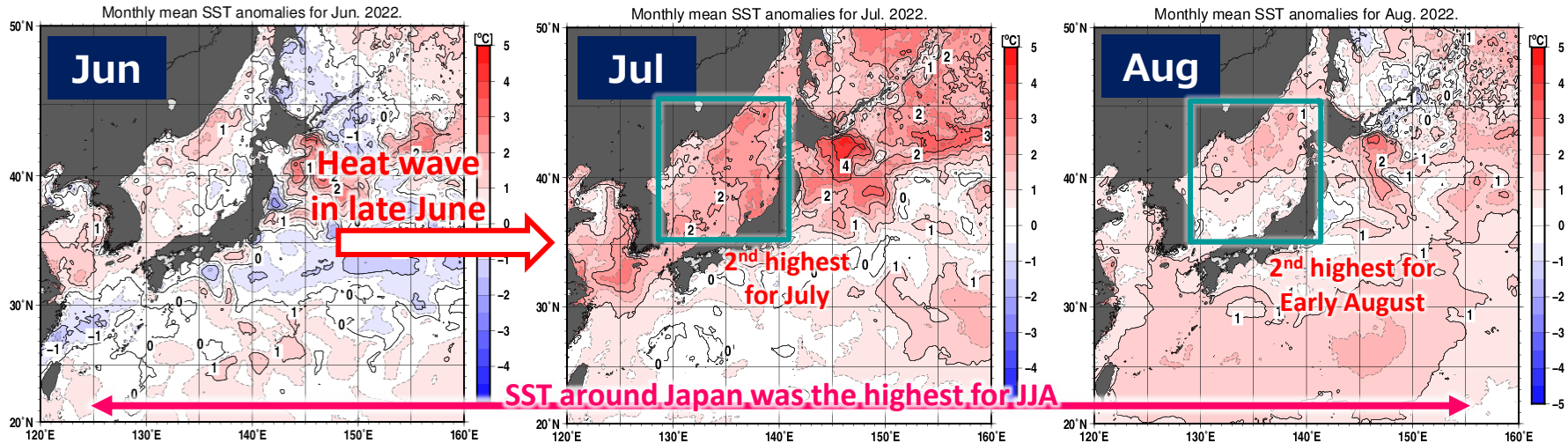
An upper level trough formed in relation to anti-cyclonic circulation over China during a month. (European blocking also affected in latter period)

# Stable front across northern Japan



The northern trough suppressed the northward migration of the front system, resulting stagnated rainband like Meiyu-Baiu across northern Japan.

# Hot SST's impacts



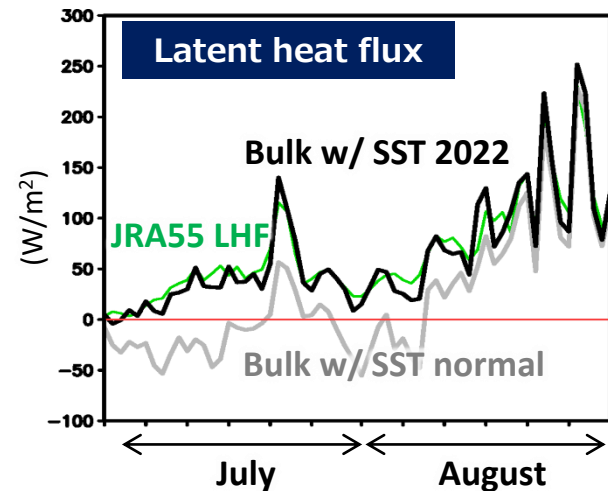
Bulk formula for latent heat

$$Q_{L1} = -\rho_a L C_E U_{10} (q_s - q_a)$$

$q_s$ : w/ SST 2022

$q_a$ : w/ SST normal

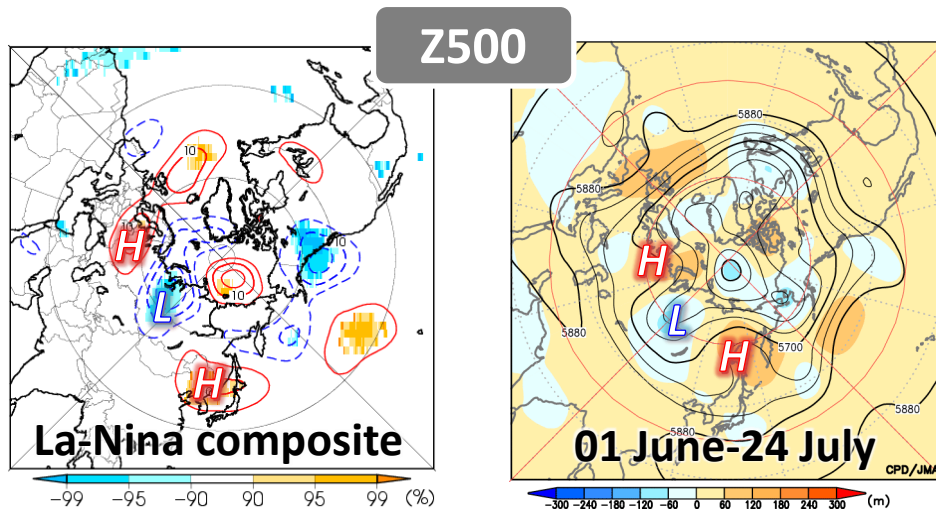
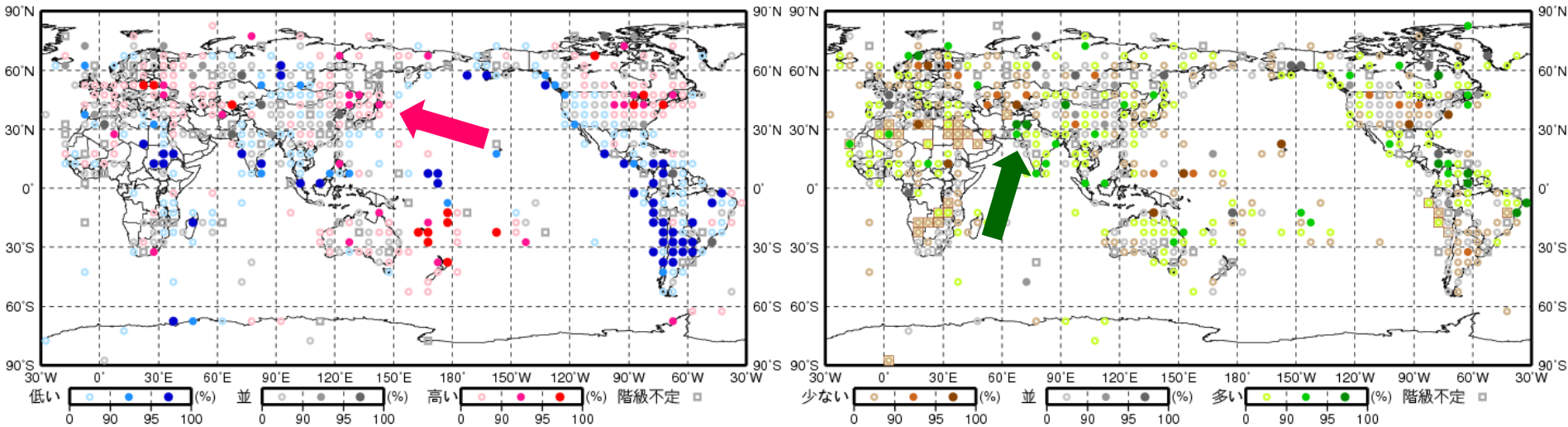
Other parameters from JRA55 and  $C_E$  from Jacobs (1942).



The hot SST in the Sea of Japan possibly supported transport of huge amount water vapor into northern Japan with less drop-out over Ocean.

# External forcings (Tropical Ocean)

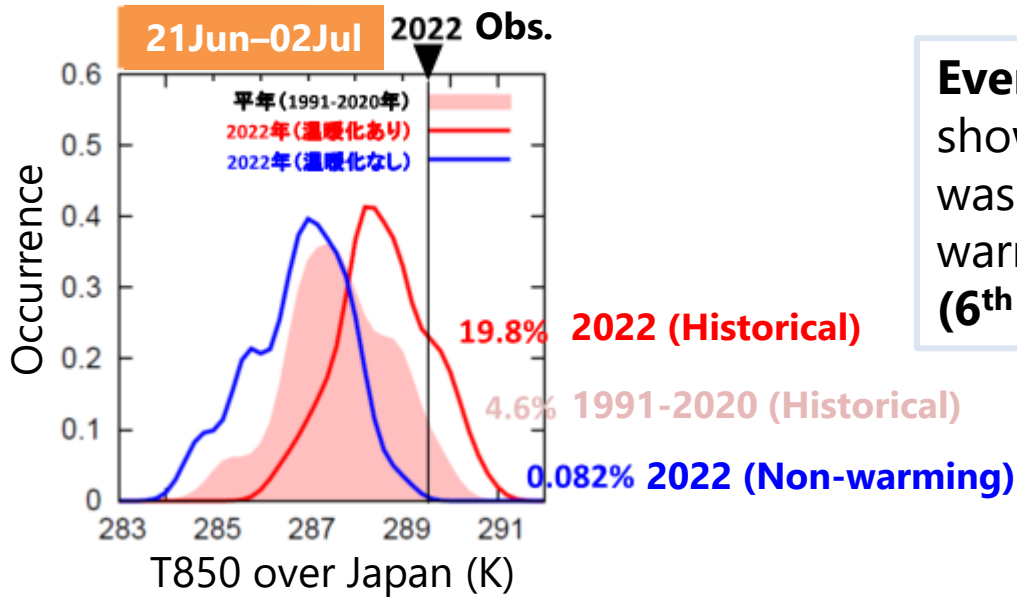
**La-Nina composite** of Temp. and Precip. in JJA based on CLIMATs.



Influences of La-Nina (as well negative IOD, not shown) seems limited.

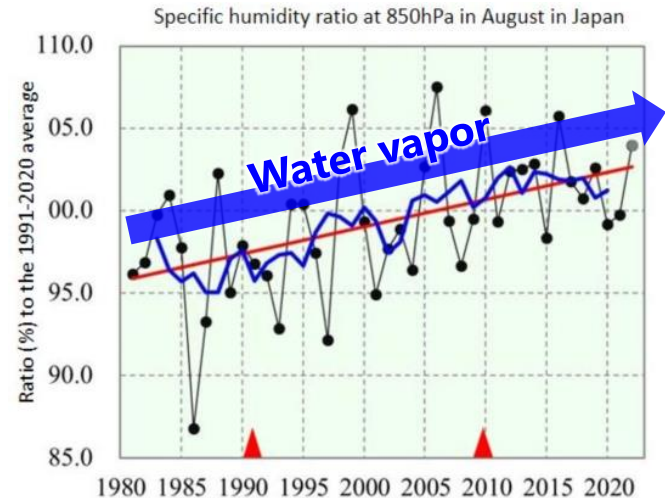
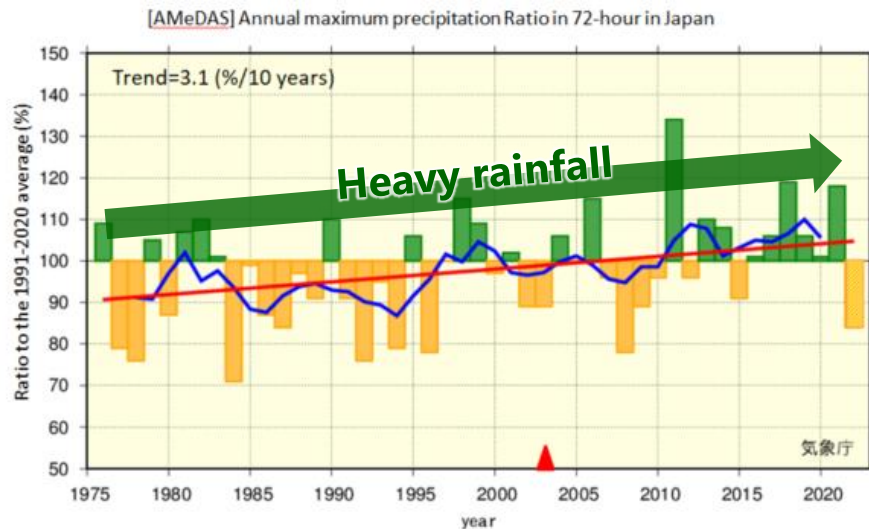
Long-lasting La-Nina (from summer 2020) may have bottom-up effect through warming NH mid- to high-latitudes (not shown).

# External forcings (Global Warming)



**Event Attribution (EA)** approach shows that the heat wave in June was highly attributable to the global warming.  
**(6<sup>th</sup> Sep Press release MEXT, MRI)**

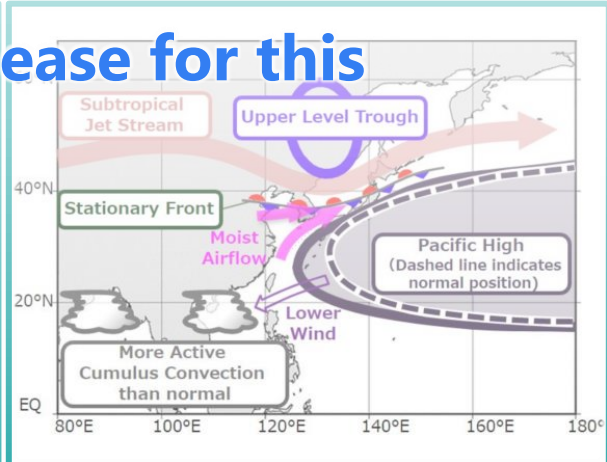
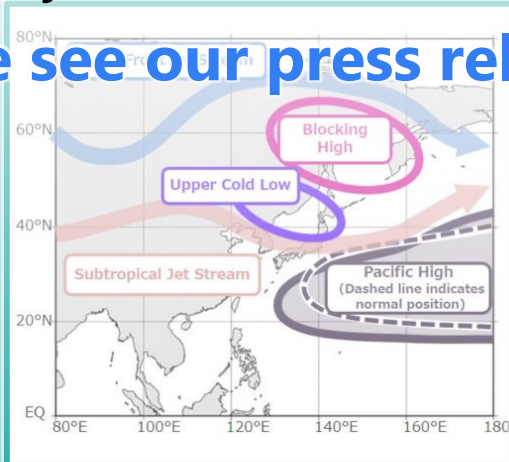
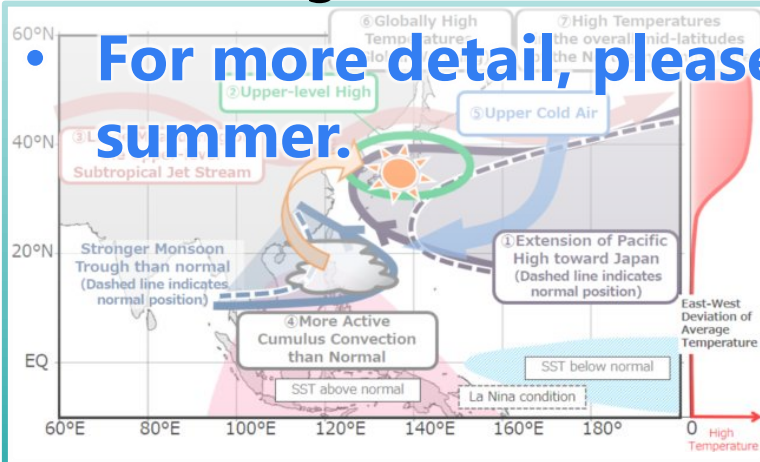
Bottom-up effect of the global warming seems evident.





- 2022 summer weather in Japan is characterized as two extremes; one is **heat wave** in June and the other is **heavy rains** in July and August.
- Dynamics (wave train, Silk-Road pattern, PJ pattern) mainly govern those extreme events, and typical influences from tropical ocean variation (i.e., La-Nina & negative IOD) seem limited.
- Bottom-up effect (i.e., warming and rich water vapor) of global warming and La-Nina may enhance those extremes.

• **For more detail, please see our press release for this summer.**

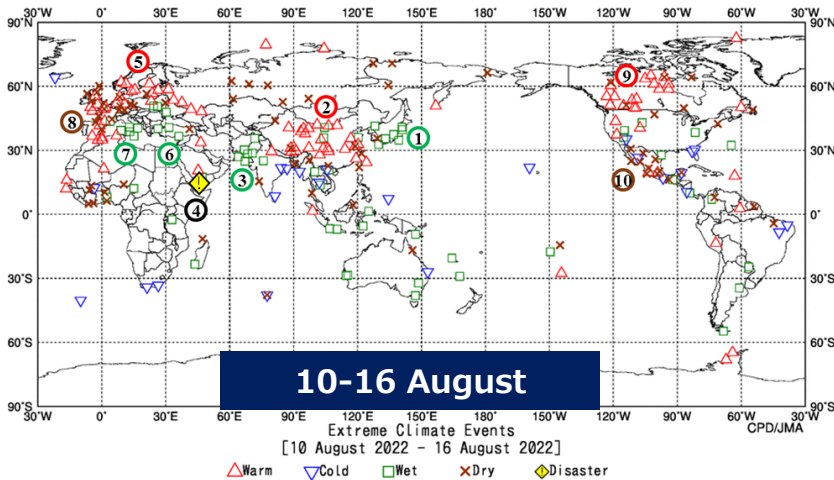
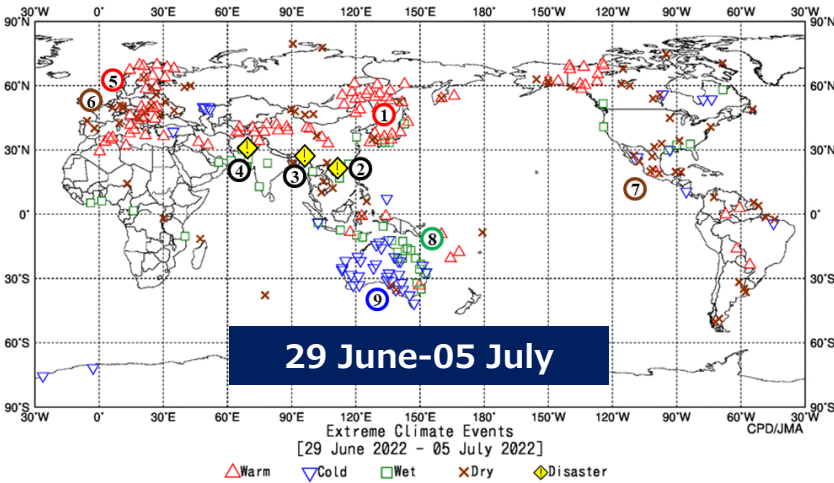


- Tokyo Climate Center <https://ds.data.jma.go.jp/tcc/tcc/index.html>
  - Climate System Monitoring <https://ds.data.jma.go.jp/tcc/tcc/products/clisys/index.html>
  - El Niño Monitoring <https://ds.data.jma.go.jp/tcc/tcc/products/elnino/index.html>
  - World Climate <https://ds.data.jma.go.jp/tcc/tcc/products/climate/index.html>
  - **Press release:** Climate characteristics and factors behind record-high temperatures in late June/early July 2022 and subsequent weather conditions [https://ds.data.jma.go.jp/tcc/tcc/news/press\\_20220914.pdf](https://ds.data.jma.go.jp/tcc/tcc/news/press_20220914.pdf)
- Takaya, K., and H. Nakamura, 2001: A Formulation of a Phase-Independent Wave-Activity Flux for Stationary and Migratory Quasi geostrophic Eddies on a Zonally Varying Basic Flow. *J. Atmos. Sci.*, **58**, 608–627.
- Kosaka, Y., and H. Nakamura, 2006: Structure and dynamics of the summertime Pacific–Japan teleconnection pattern. *QJRMS.*, **132**, 2009–2030.
- Imada, Y. et al., 2019: The July 2018 High Temperature Event in Japan Could Not Have Happened without Human-Induced Global Warming. *SOLA*, **15A**, 8–12.

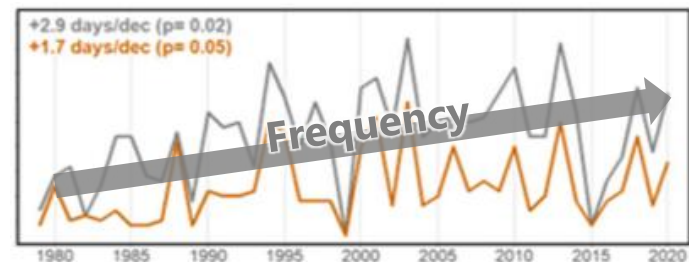
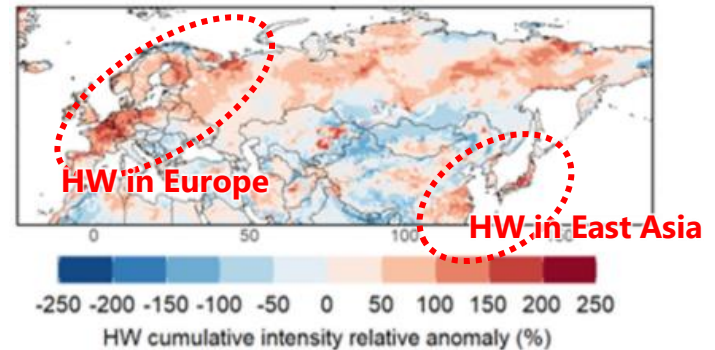
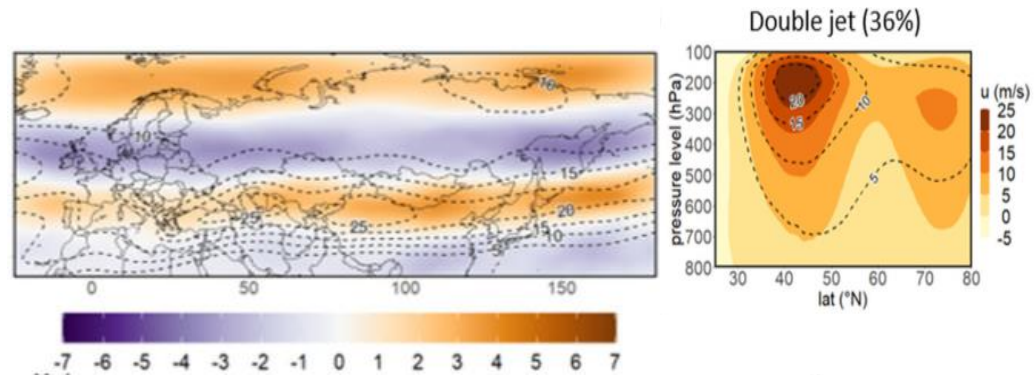
**BACKUP**

# Abnormal weather linkage

## JMA's Weekly Report on Global Extreme Climate Events

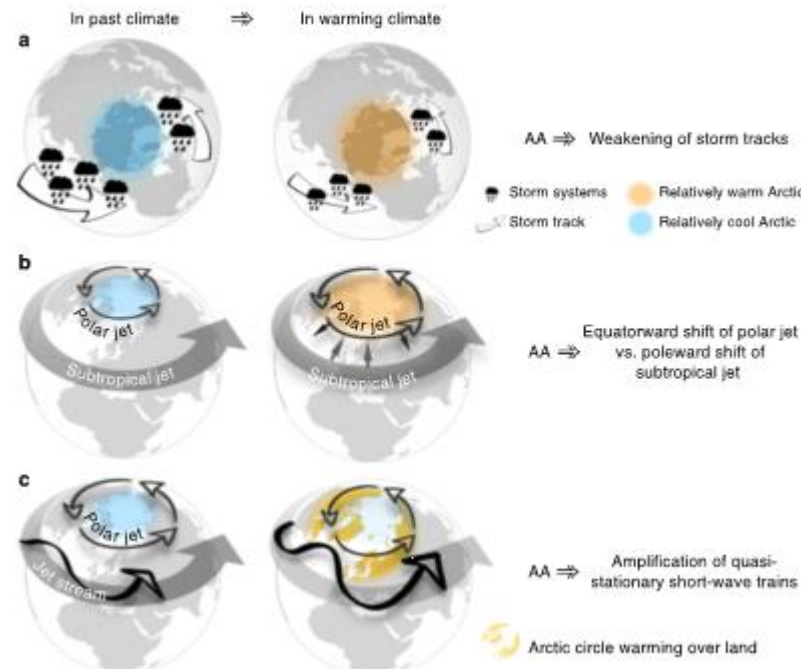
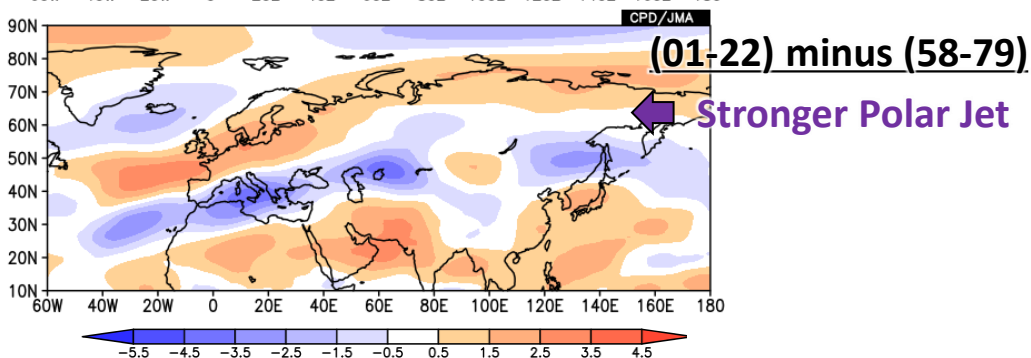
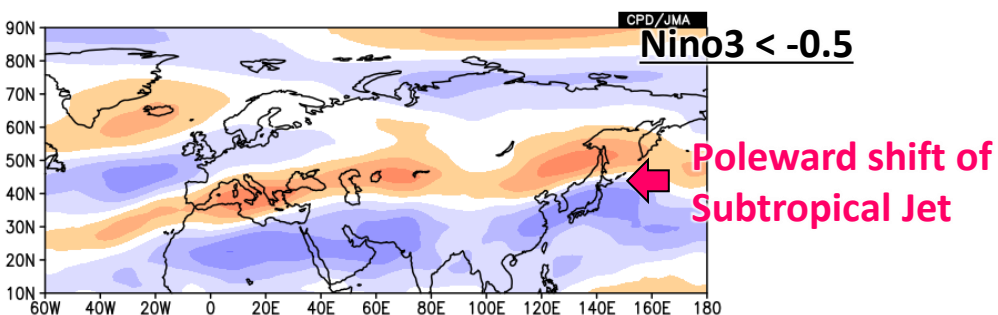
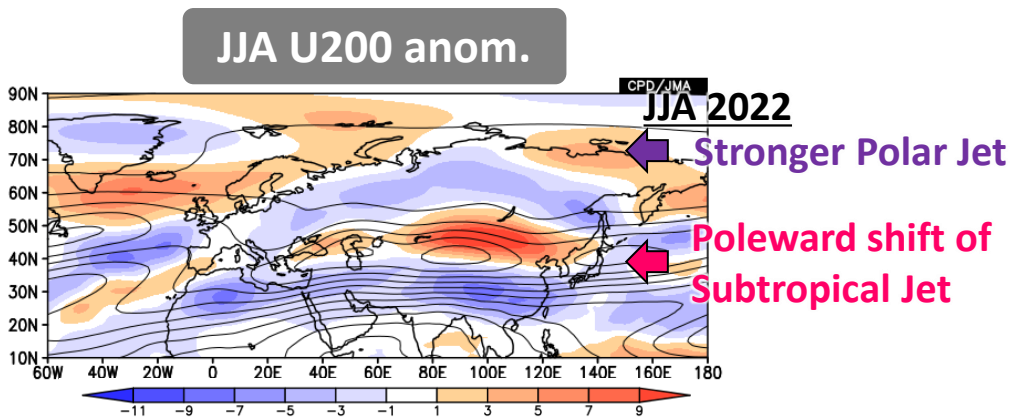


**Synchronized, suggesting Circum Global Teleconnection (CGT)**

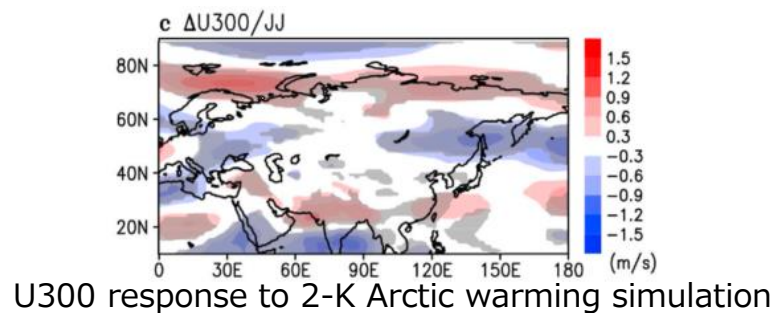


Rousi et al., 2022, NatComm

# Abnormal weather linkage

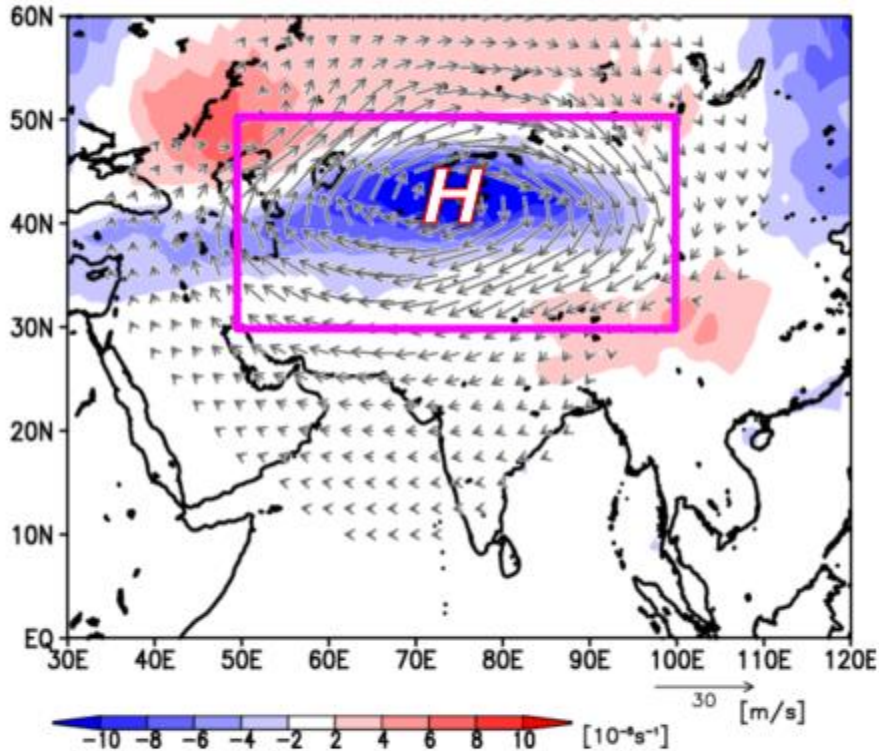


Arctic warming -> Double jet -> CGT  
Coumou et al., 2018, NatComm

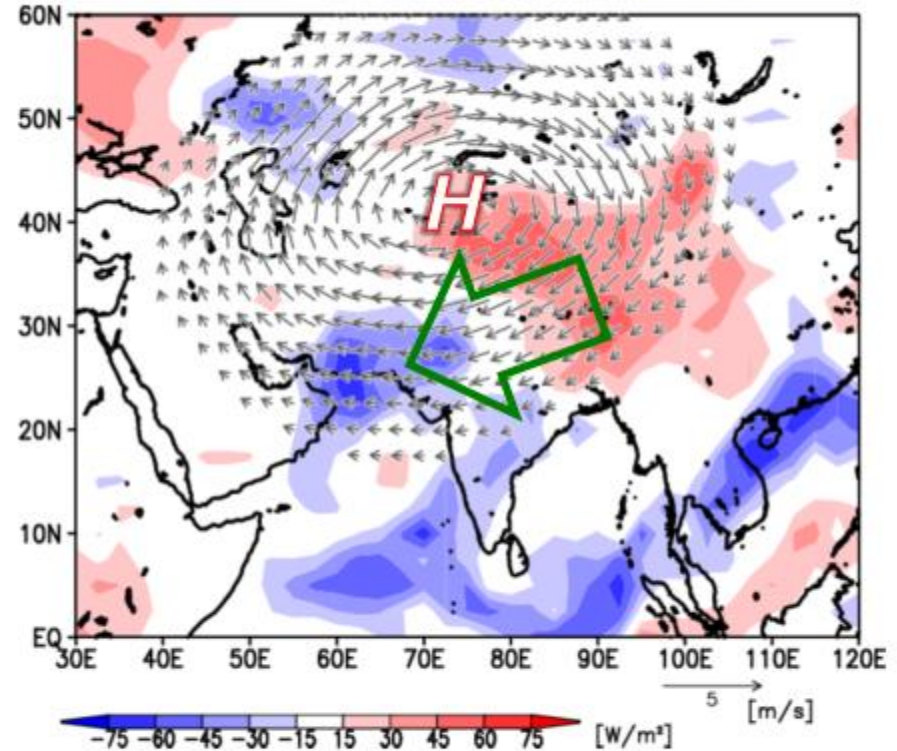


Nakamura and Sato, 2022, Env. Res.

## 200hPa循環偏差(7/1~5平均)



## 850hPa循環偏差(7/1~5平均)



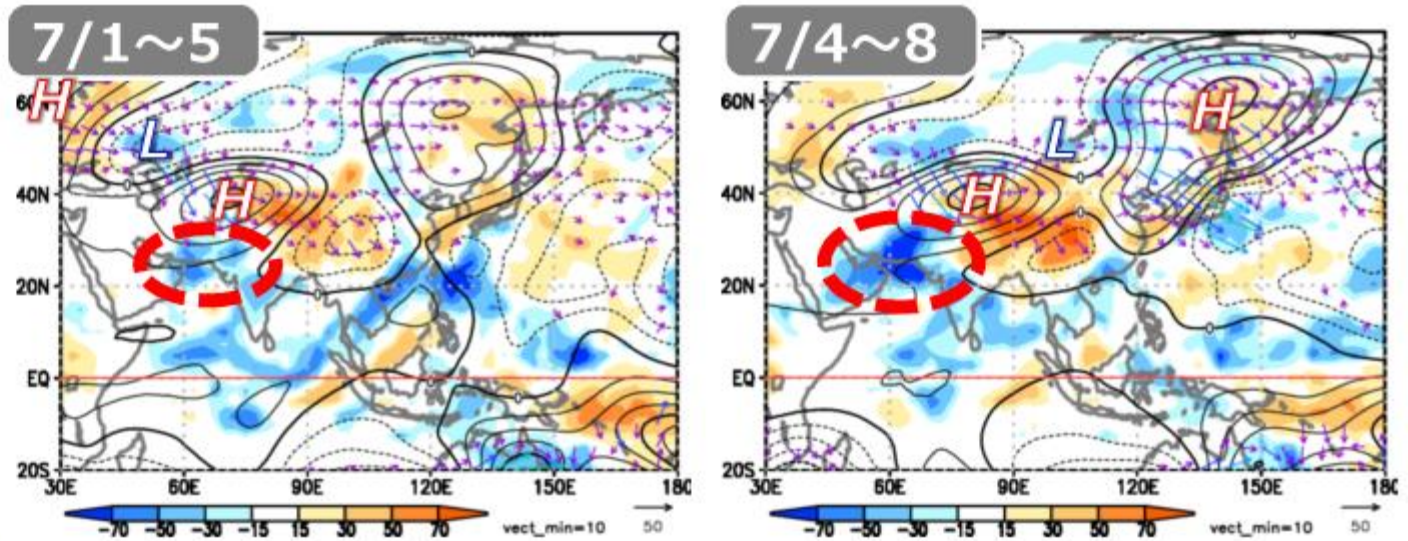
QGPV anomaly (color) and PV-induced wind anomaly (arrow) obtained by a PV inversion technique applied to 200 hPa PV anomaly.

Result suggests that upper level anti-cyclonic circulation may support to enhance rainfall over Pakistan through weakening of westerly jet over India.

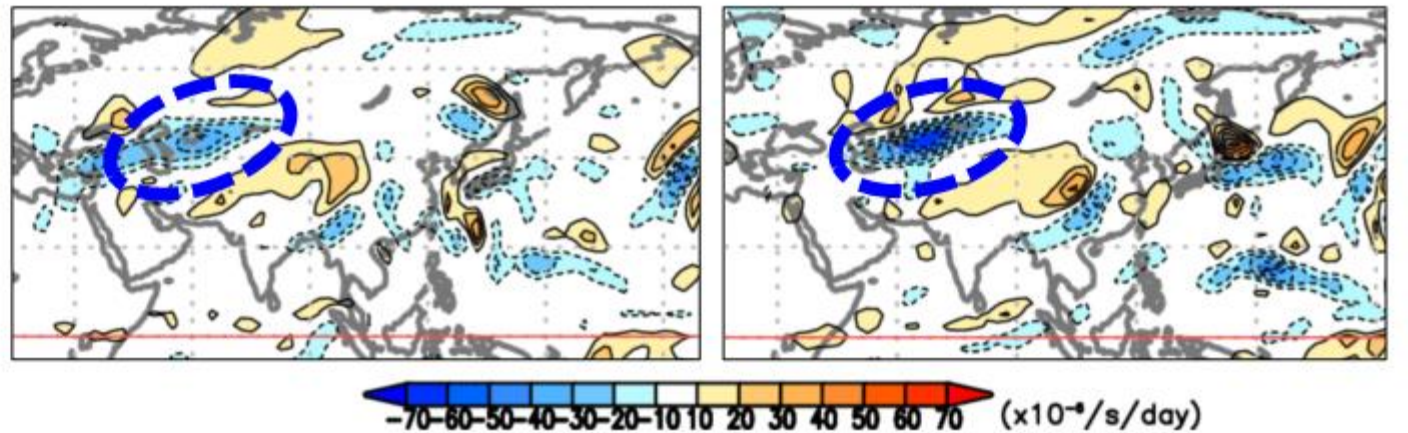
# In relation to Pakistan disaster

## $\psi$ 200平年差

等値線:  $\psi$ 200平年差  
( $10^6\text{m}^2/\text{s}$ )  
矢印: 波の活動度フラックス  
( $\text{m}^2/\text{s}^2$ ; Takaya and Nakamura 2001)  
色: OLR平年差( $\text{W}/\text{m}^2$ )



## 200hPaロスビー 波ソース (渦度移流項)

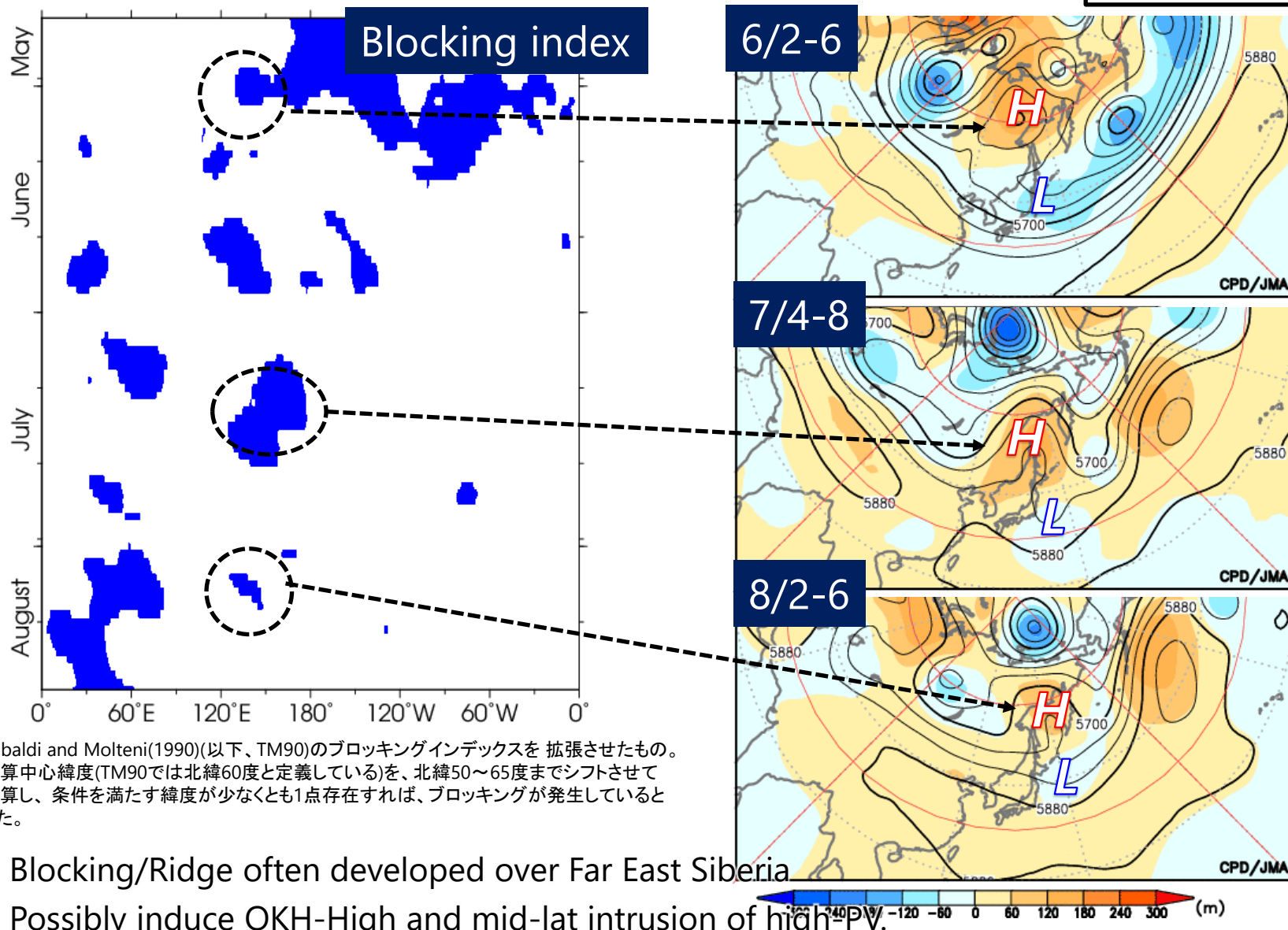


Vertical interaction (positive feedback) is suggested.

Wave train from Euro-Atlantic possibly trigger (relating to HW in Euro?).

# Blocking high

陰影: Z500偏差(m)  
コンター: Z500実況(m)



Tibaldi and Molteni(1990)(以下、TM90)のブロッキングインデックスを拡張させたもの。計算中心緯度(TM90では北緯60度と定義している)を、北緯50~65度までシフトさせて計算し、条件を満たす緯度が少なくとも1点存在すれば、ブロッキングが発生しているとした。

- Blocking/Ridge often developed over Far East Siberia
- Possibly induce OKH-High and mid-lat intrusion of high-PV.

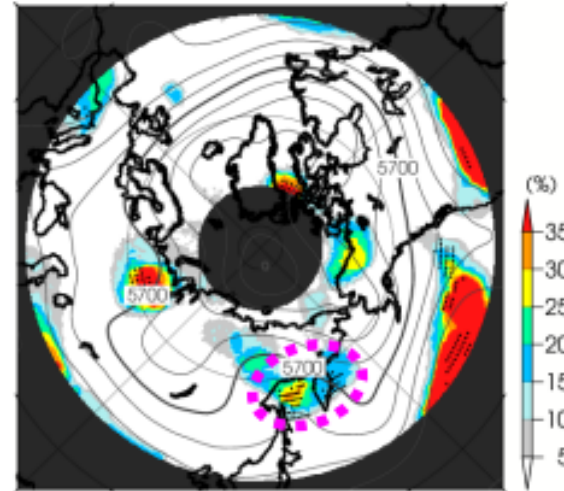


## 東シベリア南部付近でのブロッキング頻度(7/1~8/10)

7/1~8/10の期間における  
ブロッキング頻度の分布

※ブロッキング頻度は、H28年度季節予報研修テキスト  
の手法に算出した。

140~170°E, 50~60°N平均  
ブロッキング頻度の年々変動  
(各年7/1~8/10期間)



✓ オホーツク海~東シベリア南部付近のブロッキングの出現頻度は、7月~8月上旬としては  
1958年以降で最も高かった。

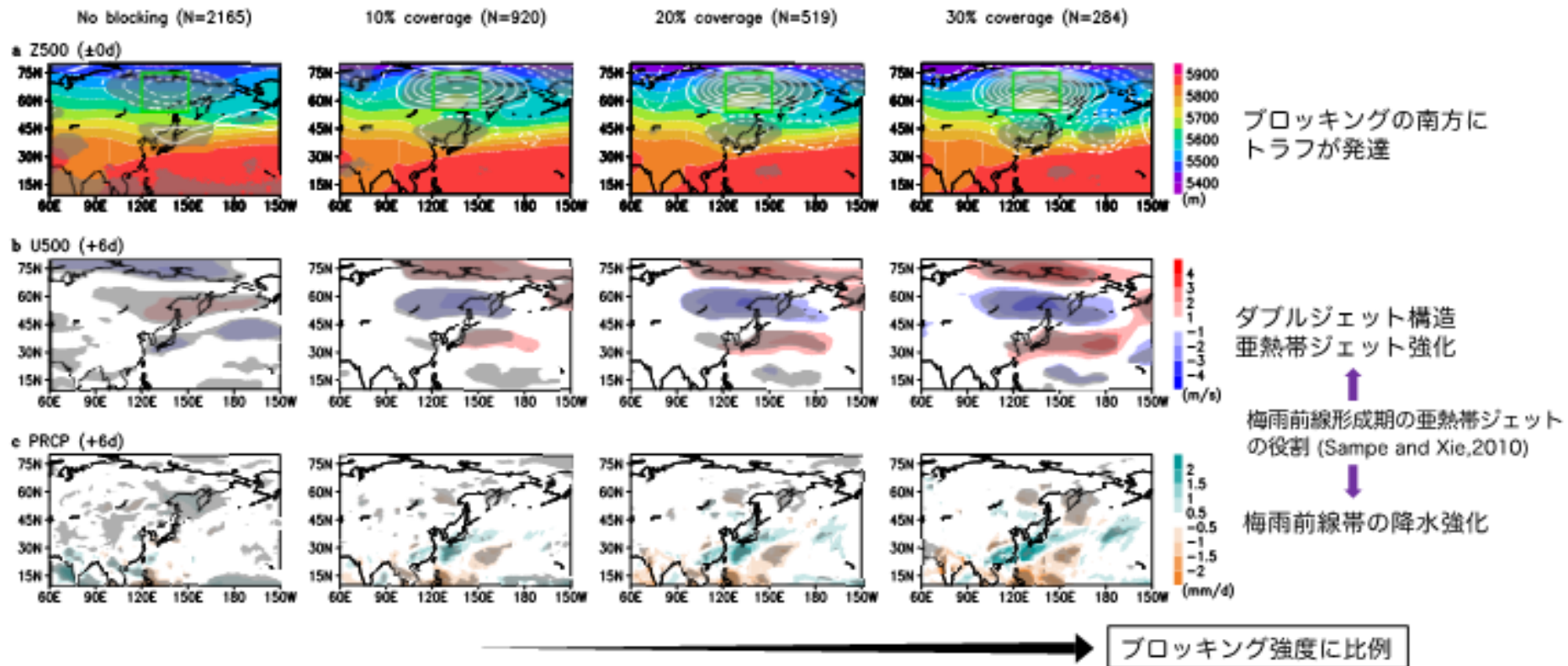
35

The **blocking-high** over the Sea of Okhotsk increases in its frequency.

## ブロッキング指数合成図

JRA55再解析（1958-2021）6-7月の11日移動平均データを使用（N=3904）

ブロッキング発生グリッドの極東シベリア平均（coverage）  $\propto$  ブロッキング強度



Nakamura and Sato, 2022, ER

## ブロッキング指数の作成

JRA55再解析（1958-2021）の11日移動平均した500hPa高度で計算

(Arai and Kimoto, 2005)

$$\frac{Z(\phi_0) - Z(\phi_s)}{\phi_0 - \phi_s} > 0 \quad \text{南方傾度}$$

$$\frac{Z(\phi_n) - Z(\phi_0)}{\phi_n - \phi_0} < \Delta Z, \quad \text{北方傾度}$$

$$\Delta Z = -8m/deg. \quad \text{しきい値}$$

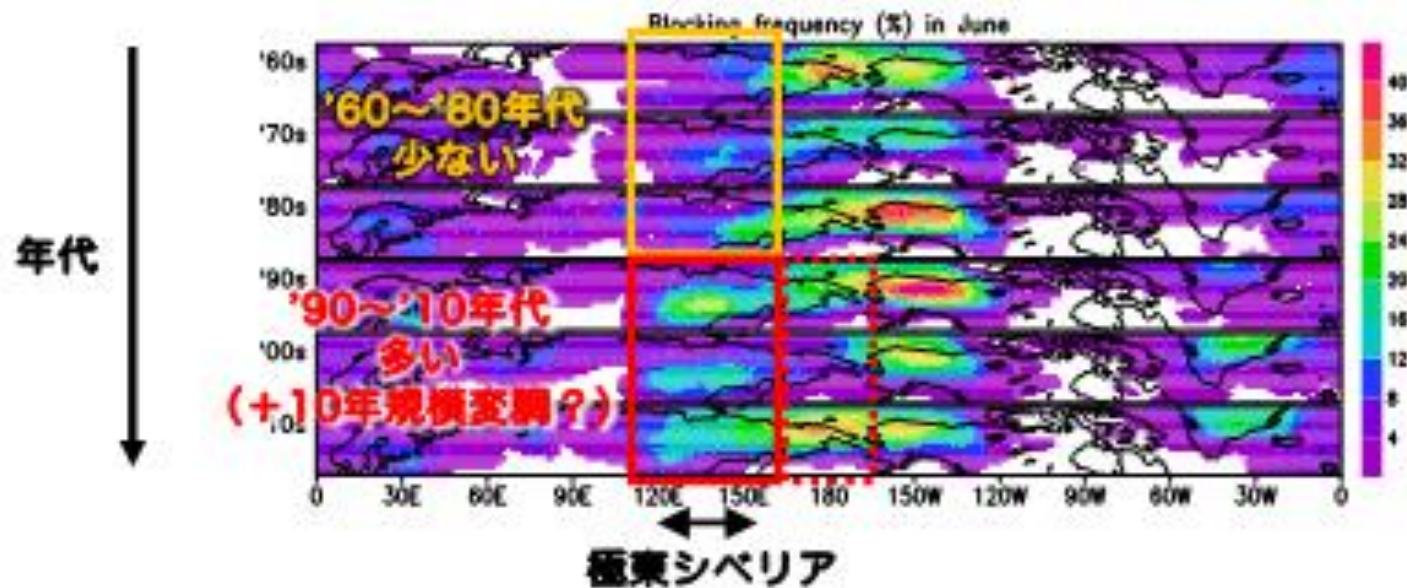
$65^{\circ}N \leq \phi_n \leq 85^{\circ}N,$   
 $50^{\circ}N \leq \phi_0 \leq 70^{\circ}N,$   
 $35^{\circ}N \leq \phi_s \leq 55^{\circ}N,$   
 緯度制限

$\Delta\phi = 15^{\circ}$

$\phi > \phi_{max}(-\partial Z/\partial y)$

亜熱帯ジェットより北側のみ

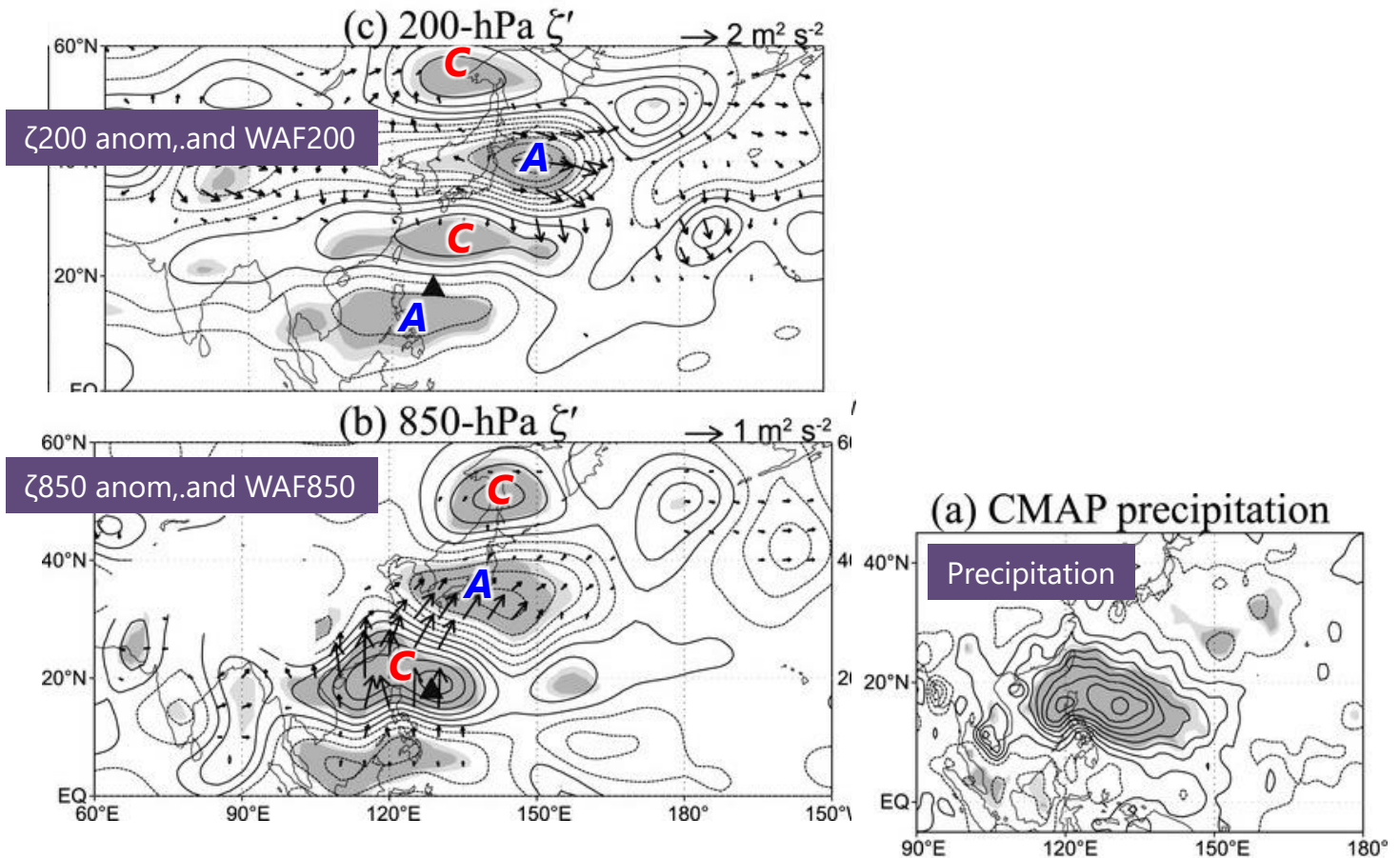
## ブロッキング指数の長期変化（現在）



- The Pacific-Japan (PJ) pattern (eg., Nitta (1987), Kosaka and Nakamura (2010))

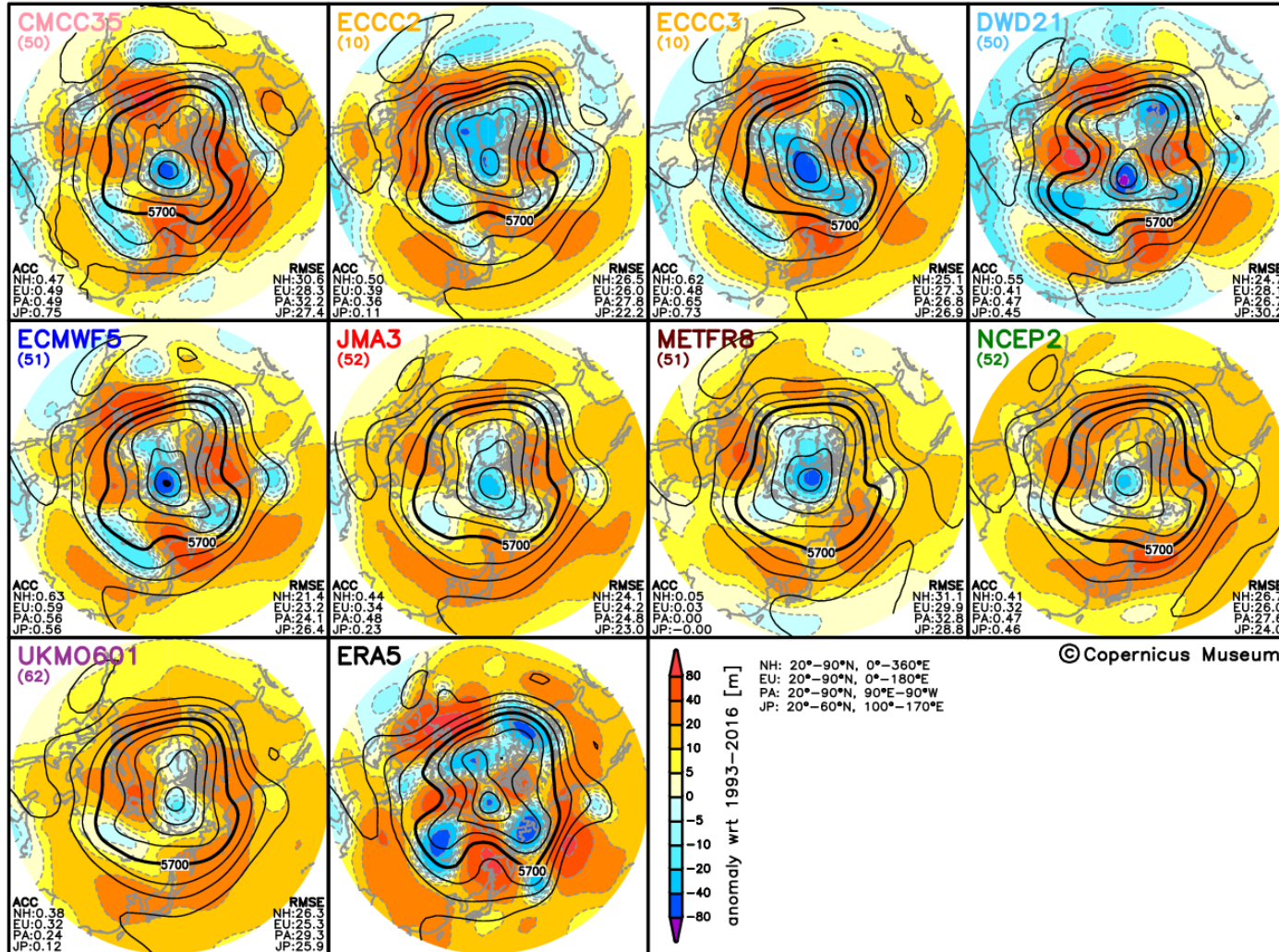
## PJ Composites

Kosaka and Nakamura (2010)  
\*“C” and “A” superimposed



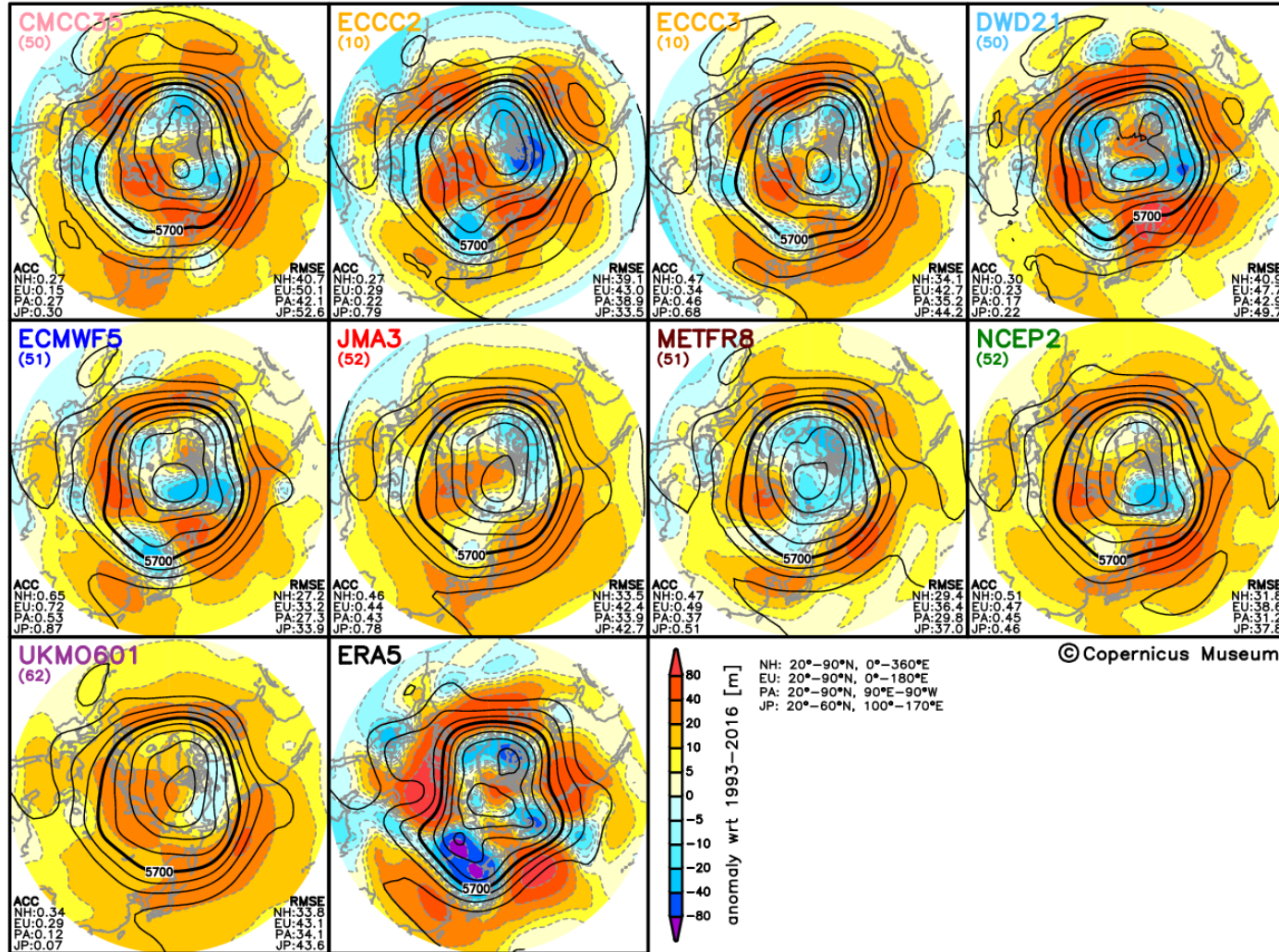
## Seasonal forecasts (Z500 ensemble mean)

Initial: 2022.07.01, Valid: 2022.07.01–2022.07.31 (Mon1)



## Seasonal forecasts (Z500 ensemble mean)

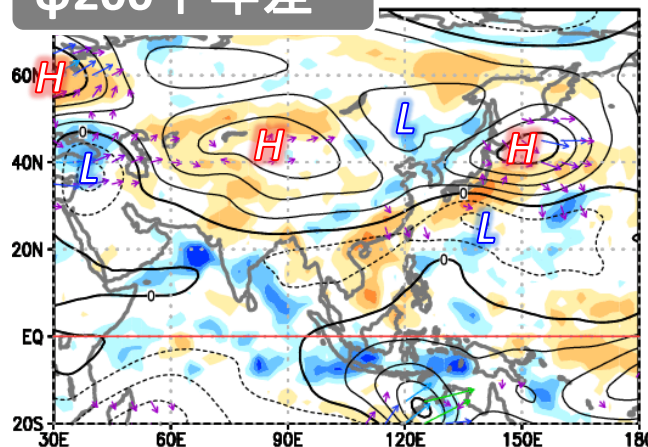
Initial: 2022.08.01, Valid: 2022.08.01–2022.08.31 (Mon1)



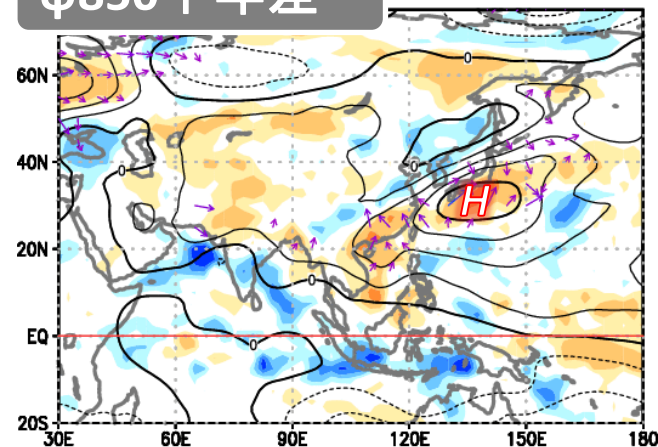
# Circulation anomalies during hot events

6/23~27平均場

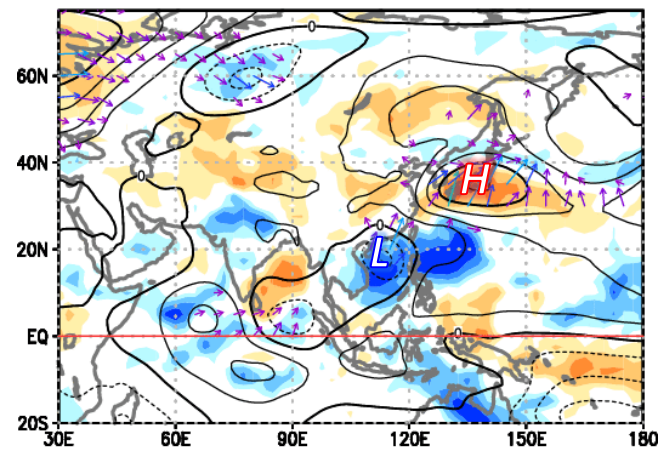
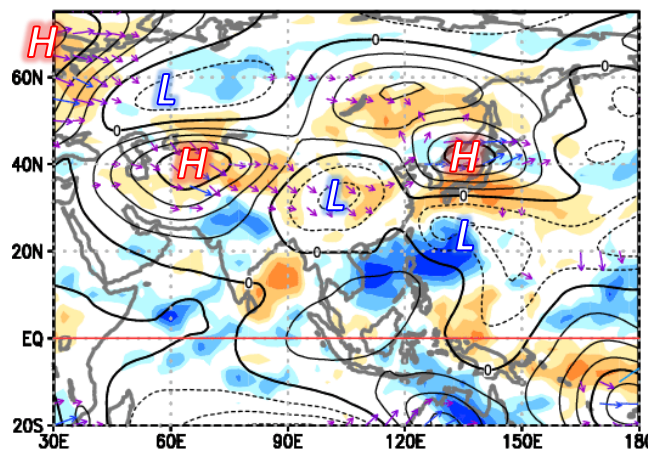
ψ200平年差



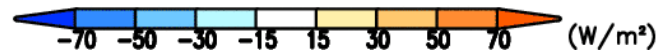
ψ850平年差



6/28~7/2平均場



等値線: 流線関数平年差( $10^6 \text{m}^2/\text{s}$ )  
 矢印: 波の活動度フラックス( $\text{m}^2/\text{s}^2$ )  
 ※Takaya and Nakamura (2001)  
 陰影: OLR平年差( $\text{W}/\text{m}^2$ )

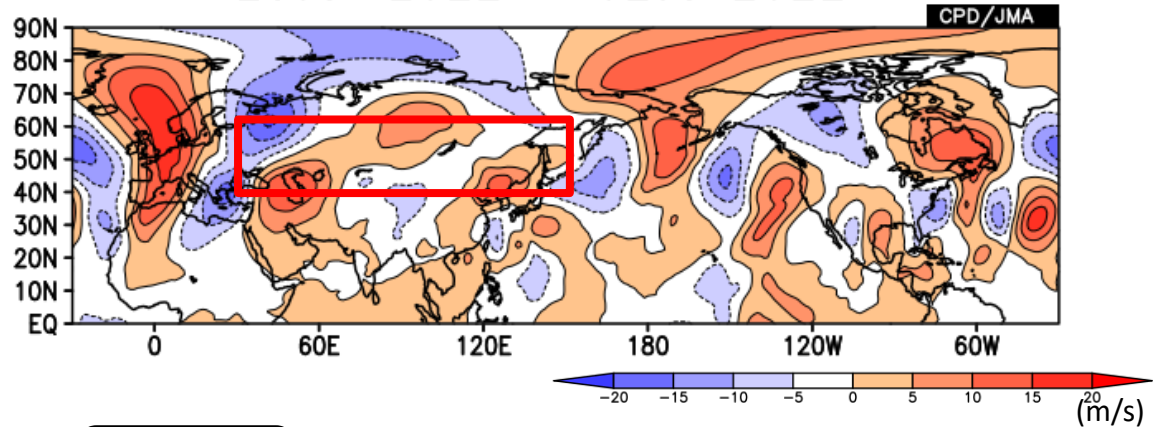


- ✓ アジアジェット気流に沿う波束伝播に伴って、日本付近の上層では高気圧性循環偏差が持続。下層でも、日本の南海上を中心に高気圧性循環偏差。
- ✓ 期間後半にはPJパターンも出現し、日本付近での下層高気圧性循環偏差の維持に寄与。

# Meandering of Asia Jet

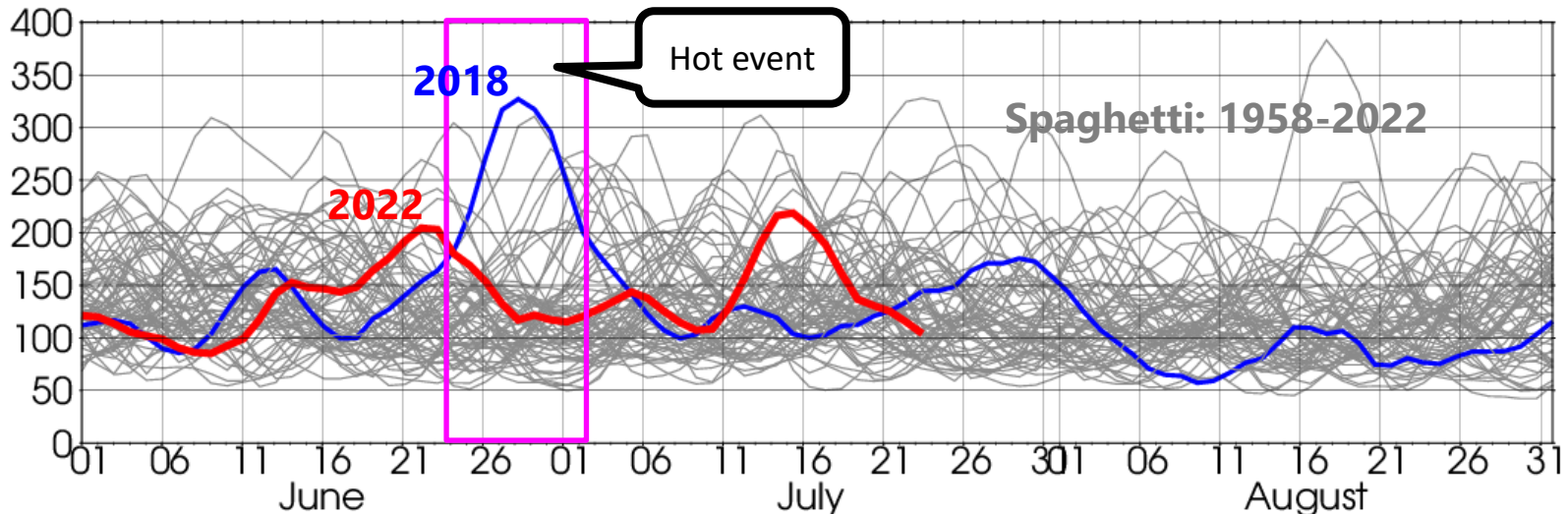
6/23~7/2平均  
V200 anom (m/s)

23Jun.2022 - 02Jul.2022



V200 square

(m<sup>2</sup>/s<sup>2</sup>)



赤線: 2022年、青線: 2018年、灰色線: 1958年以降のその他の年  
5日移動平均  
単位: m<sup>2</sup>/s<sup>2</sup>

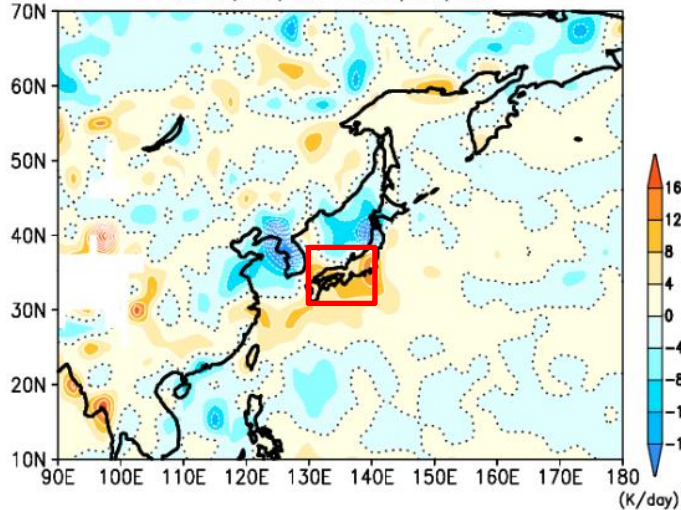
✓ Meandering was not strong



## Vertical advection 850hPa

(f) 鉛直流による気温の鉛直移流 (全項)

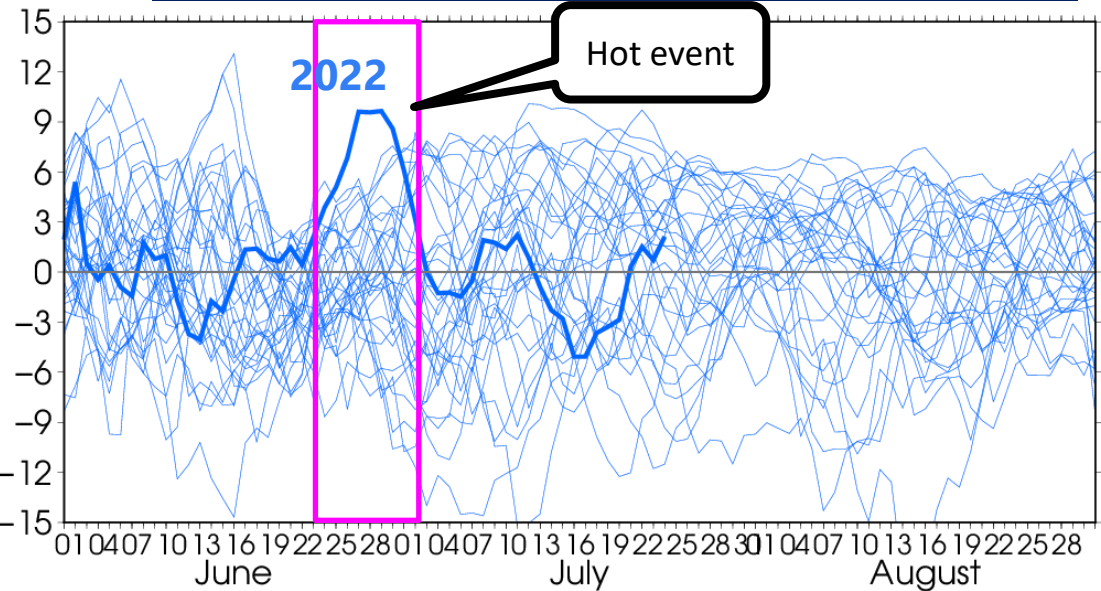
$\text{Omg} \times T$  (anom total) @850hPa  
2022/06/23-2022/07/02



色: 850hPa鉛直流偏差による気温平年値移流 (K/day)

## Vertical advection (850hPa,30-38N,130-140E)

(K/day)



太線: 2022年、細線: 1958~2021年  
5日移動平均  
単位: K/day

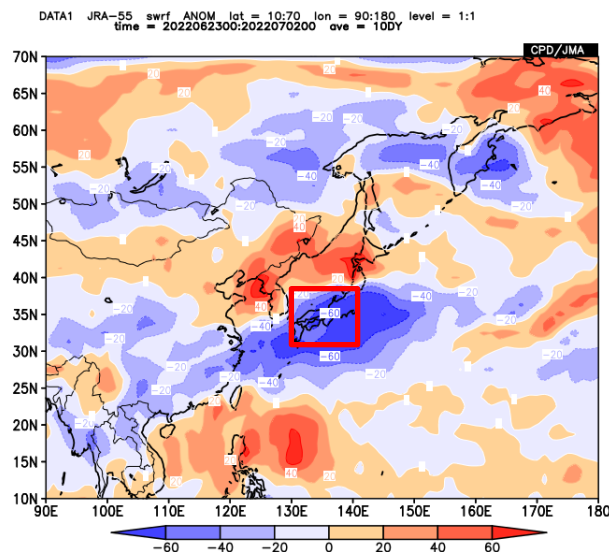
- ✓ Adiabatic heating due to strong downward motion is the largest among records for late June in eastern and western Japan.

## 熱力学方程式 (気温偏差に関する平年値と平年偏差に分離)

$$\frac{\partial T'}{\partial t} = \frac{Q}{C_p} - \mathbf{u}' \cdot \nabla \bar{T} - \bar{\mathbf{u}} \cdot \nabla T' - \mathbf{u}' \cdot \nabla T' - \left( \frac{p}{p_0} \right)^{\frac{R}{C_p}} \bar{\omega}' \frac{\partial \bar{\theta}}{\partial p} - \left( \frac{p}{p_0} \right)^{\frac{R}{C_p}} \bar{\omega} \frac{\partial \theta'}{\partial p} - \left( \frac{p}{p_0} \right)^{\frac{R}{C_p}} \omega' \frac{\partial \theta'}{\partial p}$$

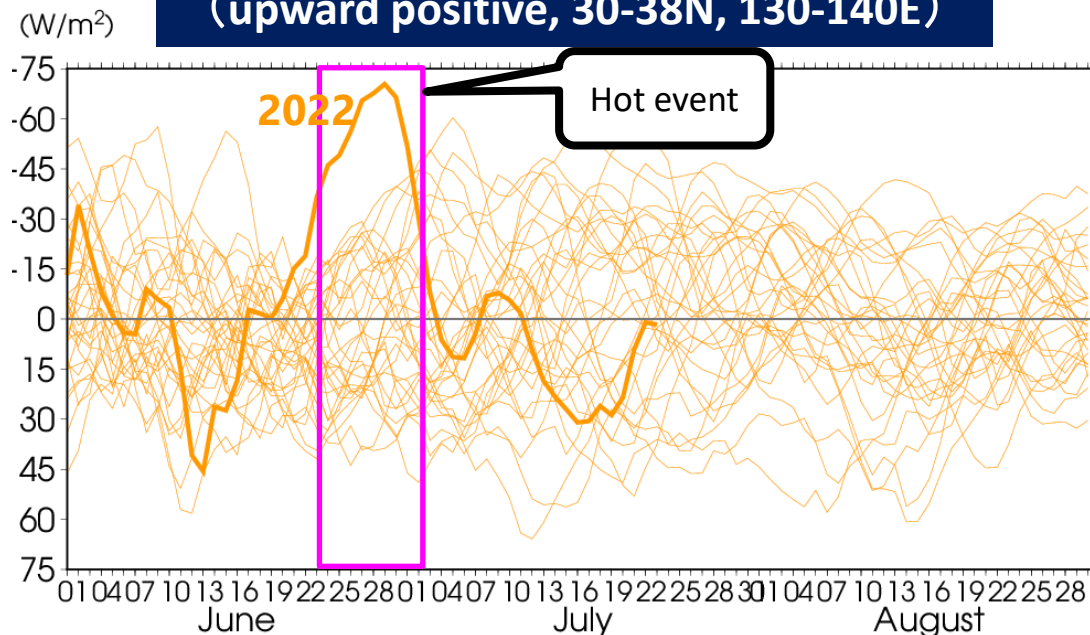
# Short wave radiation heating

## SW radiation flux anom. (upward positive)



色: 短波放射フラックス偏差 (W/m<sup>2</sup>)

## SW radiation flux (upward positive, 30-38N, 130-140E)



太線: 2022年、細線: 1958~2021年  
5日移動平均  
単位: W/m<sup>2</sup>

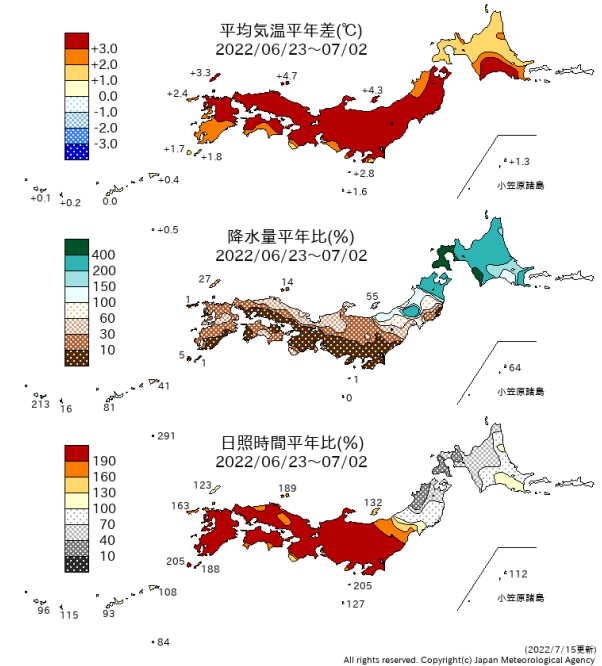
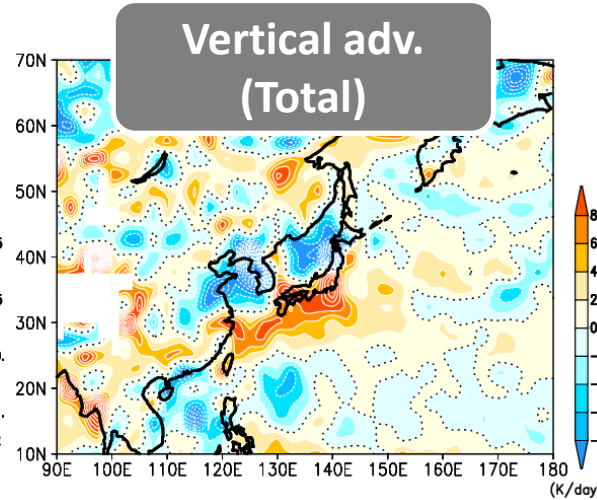
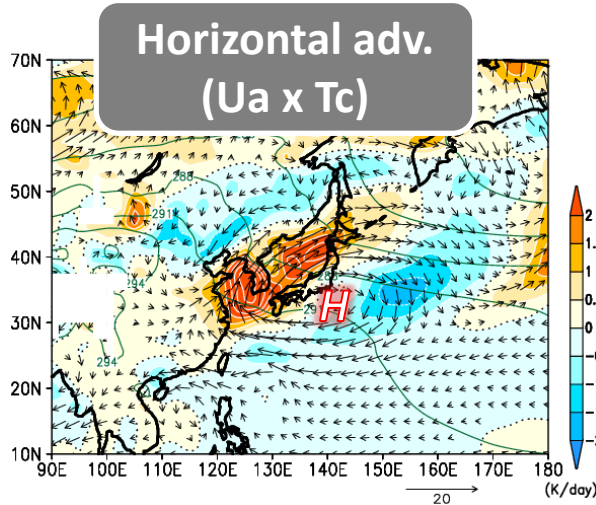
✓ Radiative heating due to SW radiation (sunniness) is the largest as well.

熱力学方程式(気温偏差に関する平年値と平年偏差に分離)

$$\frac{\partial T'}{\partial t} = \frac{Q}{C_p} - \mathbf{u}' \cdot \nabla \bar{T} - \bar{\mathbf{u}} \cdot \nabla T' - \mathbf{u}' \cdot \nabla T' - \left(\frac{p}{p_0}\right)^{\frac{R}{C_p}} \omega' \frac{\partial \bar{\theta}}{\partial p} - \left(\frac{p}{p_0}\right)^{\frac{R}{C_p}} \bar{\omega} \frac{\partial \theta'}{\partial p} - \left(\frac{p}{p_0}\right)^{\frac{R}{C_p}} \omega' \frac{\partial \theta'}{\partial p}$$

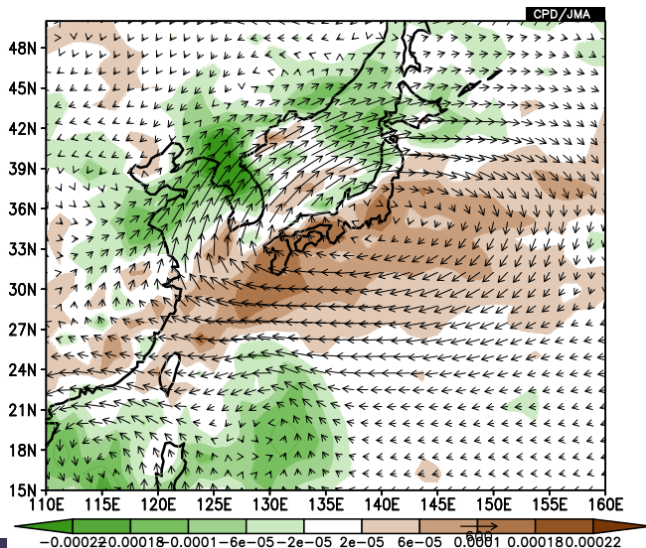
## Heat budget 850hPa

左図の矢印: 風平年差(m/s)  
 緑線: 気温平年値(K)



## Vertically integrated water vapor flux and its Div.

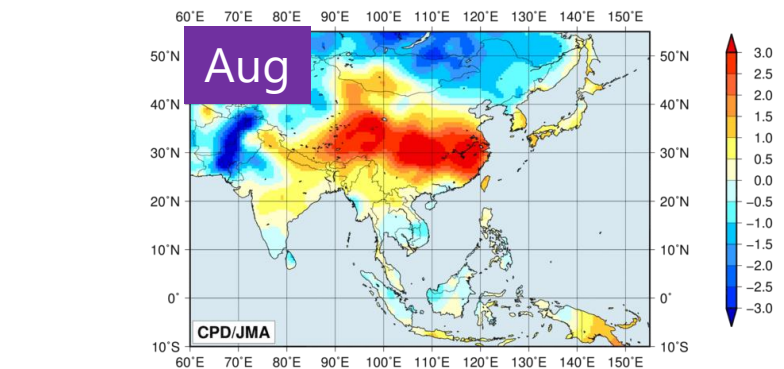
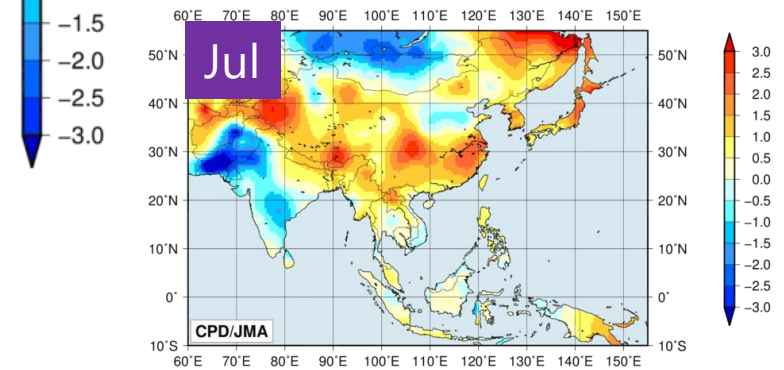
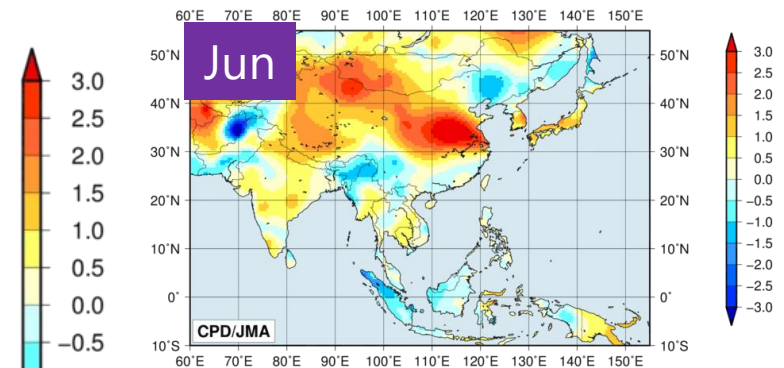
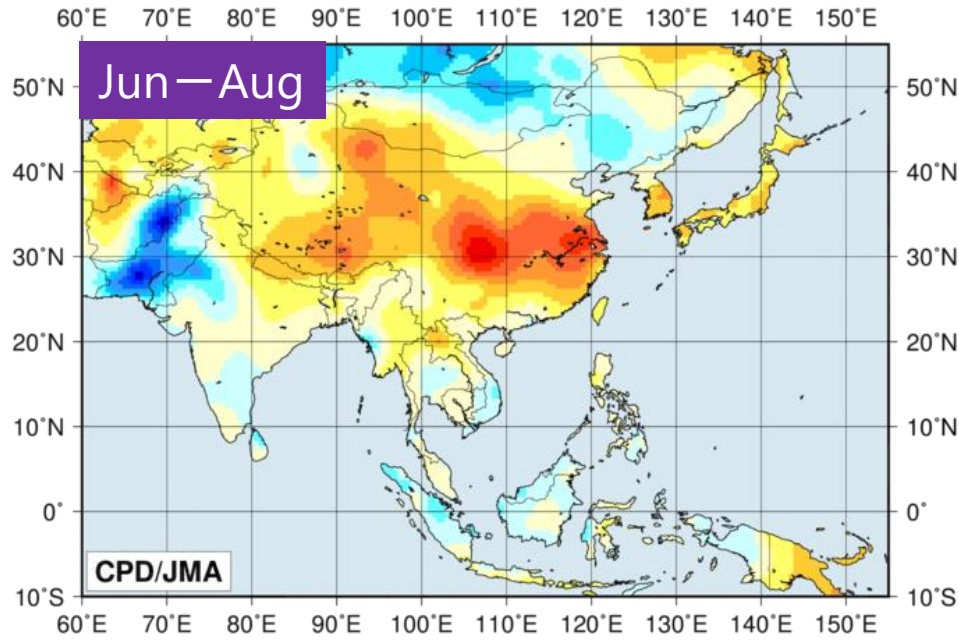
矢印: 水蒸気フラックス(kg/m/s)  
 陰影: 水蒸気フラックスの収束発散(kg/m<sup>2</sup>/s)  
 ※1000~300hPaで鉛直積算



- ✓ In and around Northern Japanでは、太平洋高気圧の周縁に沿う暖気移流偏差や湿った空気の流入が明瞭で、**warm・wet**となった。
- ✓ In and around Western and Eastern Japanでは、高気圧付近での断熱加熱偏差が明瞭で、湿った気流の影響を受けにくく、**warm・dry・sunniness**となった。

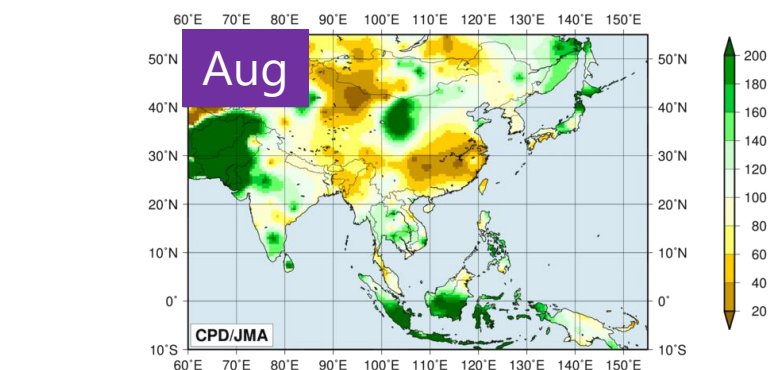
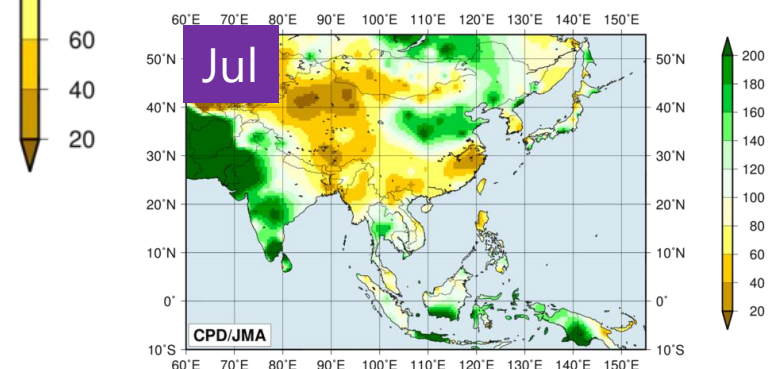
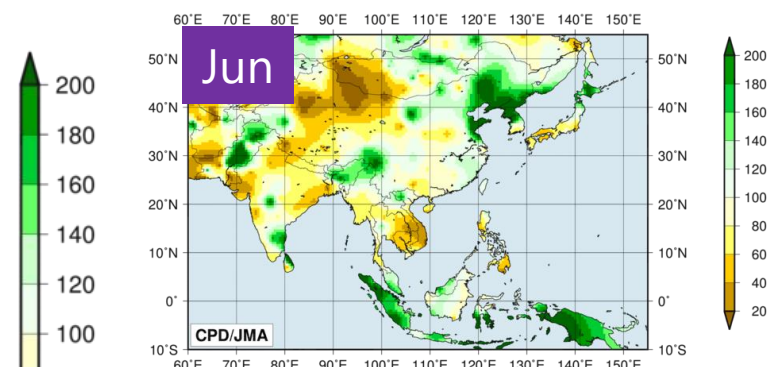
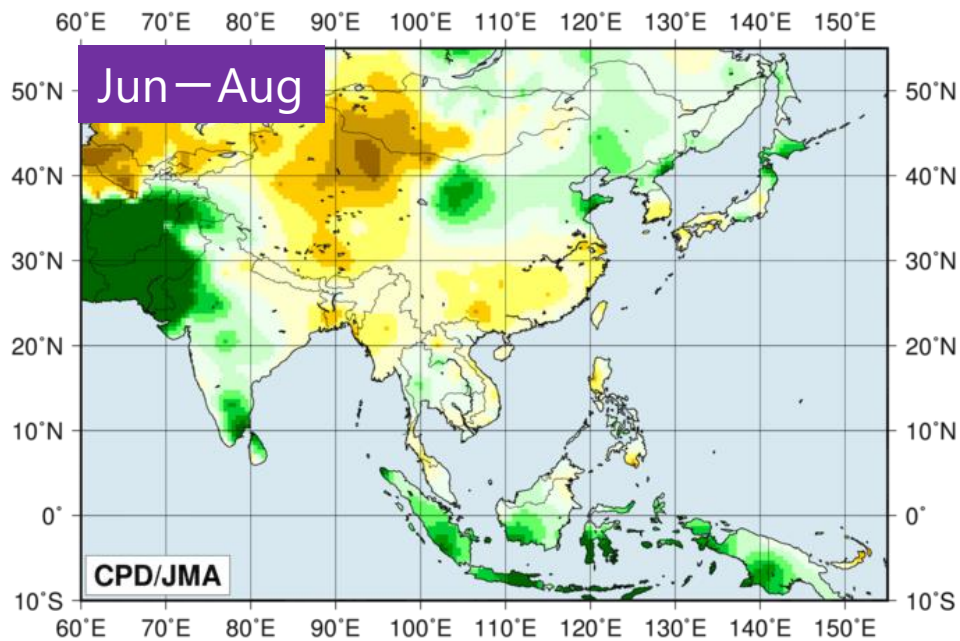
# Temperature anom. in 2022 summer

\*Based on CLIMAT reports. Reference period for anomaly is 1991-2020.

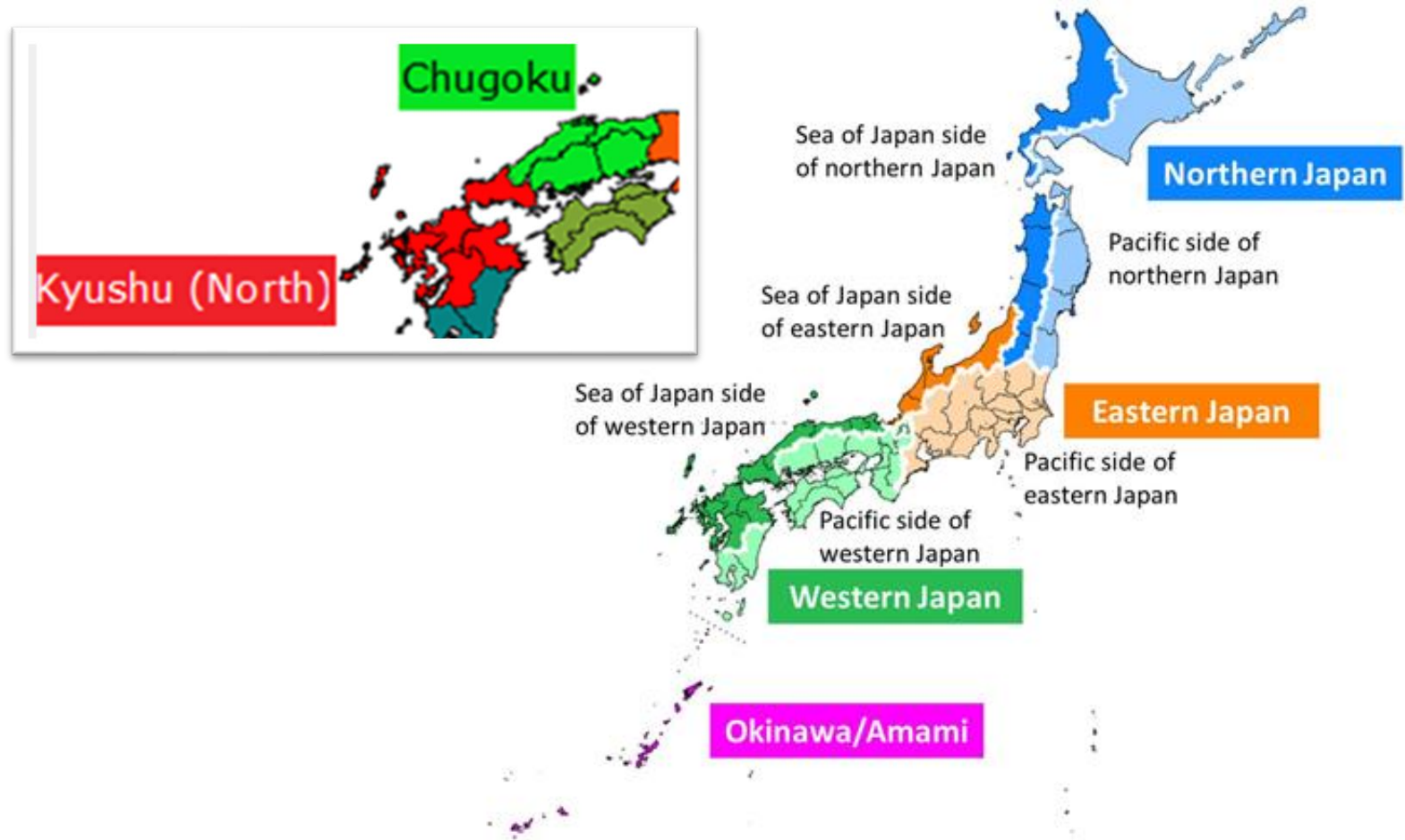


# Precipitation ratio in 2022 summer

\*Based on CLIMAT reports. Reference period for ratio is 1991-2020.

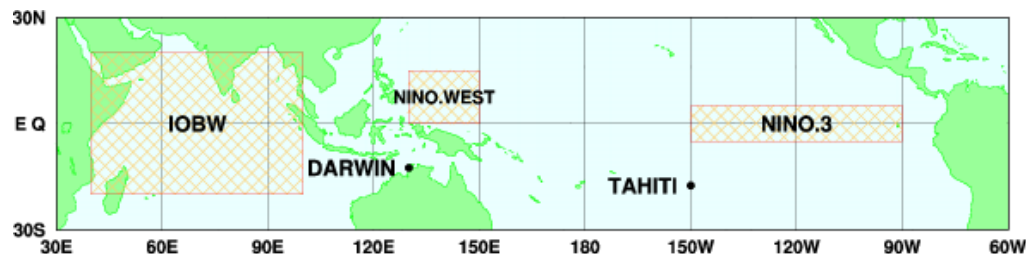


# Regions of Japan

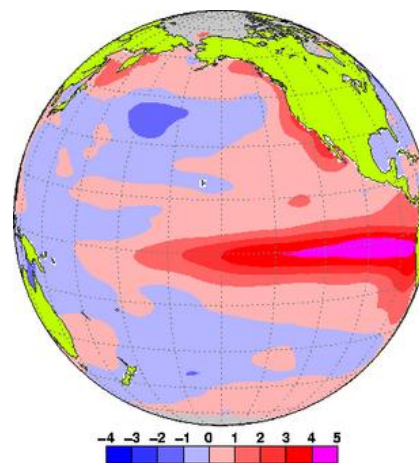
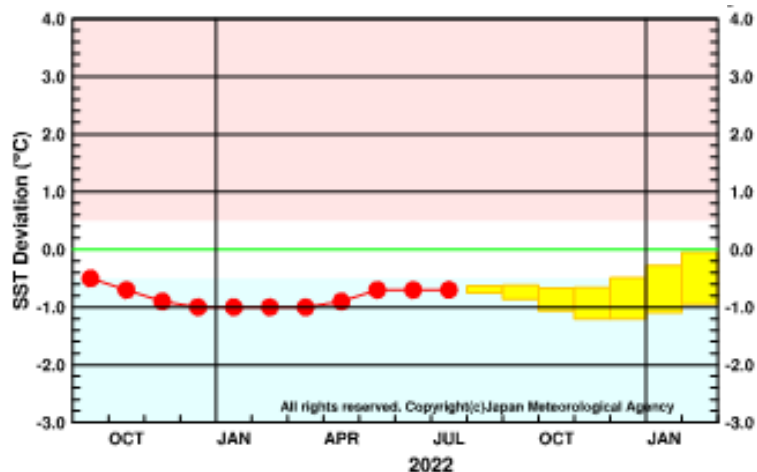


# Definition: ENSO

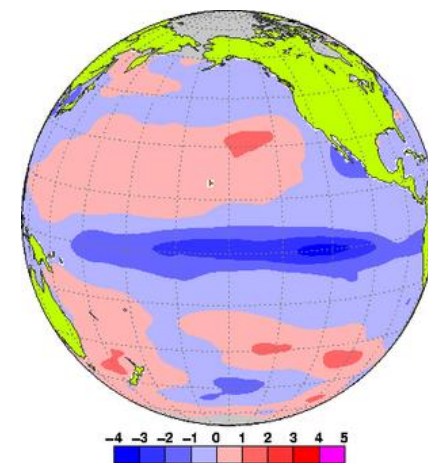
The definition of El Niño(La Niña) is such that the 5-month running mean Sea Surface Temperature (SST) deviation for NINO.3(5°S-5° N,150°W-90°W) continues 0.5°C(-0.5°C) or higher (lower) for 6 consecutive months or longer. The NINO.3 SST deviation is defined as deviation from the latest sliding 30 year.



La-Nina continues



El Niño  
SST anoms. in Nov. 1997



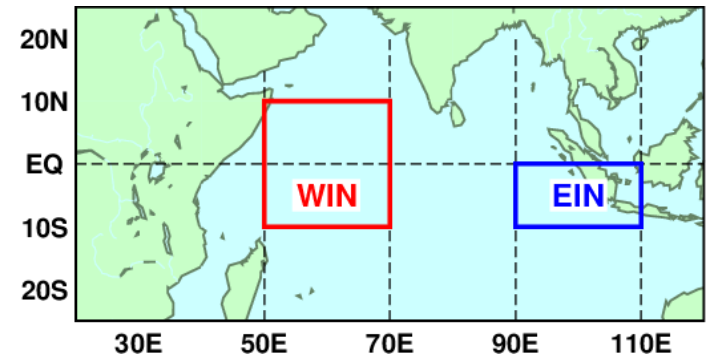
La Niña  
SST anoms. in Dec. 1988

# Definition: IOD

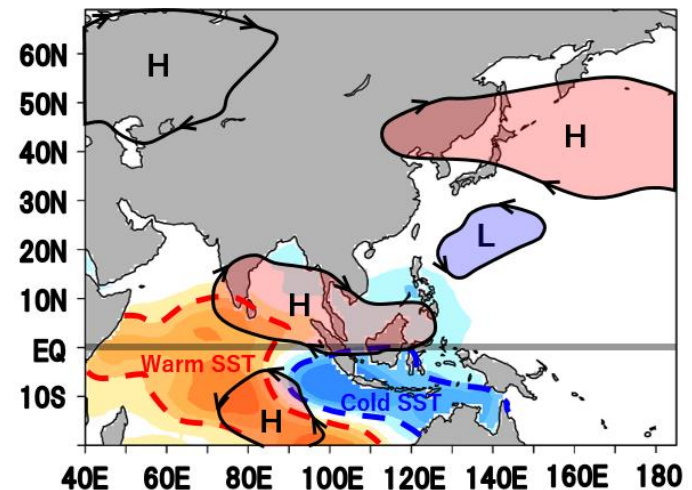
**Dipole mode index (DMI)**  
**= WIN SST minus EIN SST**

Differences in area-averaged monthly-mean SST deviations between **the tropical western Indian Ocean [50° - 70°E, 10°S- 10°N] (denoted as the WIN area)** and **the southeastern tropical Indian Ocean [90 - 110°E, 10°S - Equator] (denoted as the EIN area)**, with monthly-mean SST deviation based on linear extrapolation with respect to the latest sliding 30-year mean for each calendar month.

Positive (negative) IOD events are identified when the three-month running mean DMI is +0.4 °C or above (-0.4 °C or below) for at least three consecutive months between June and November.

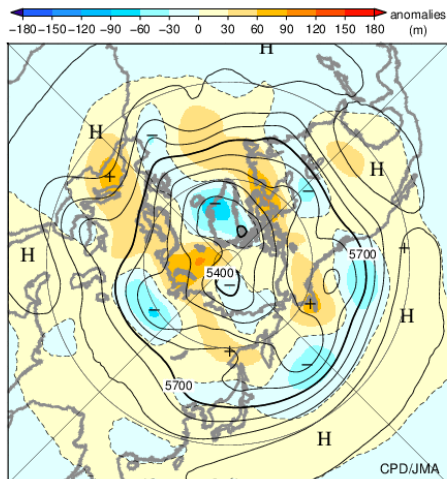


Typical anomalies SST and low-level circulation associated with positive IOD



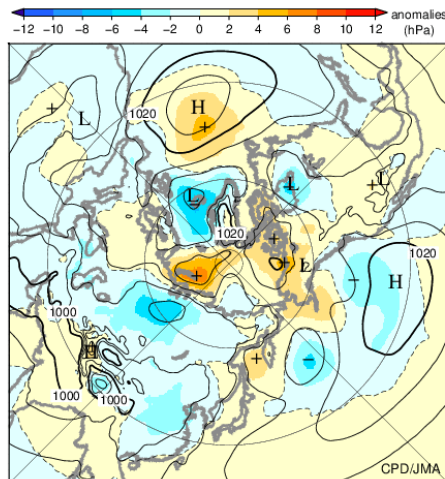


## z500 anom.



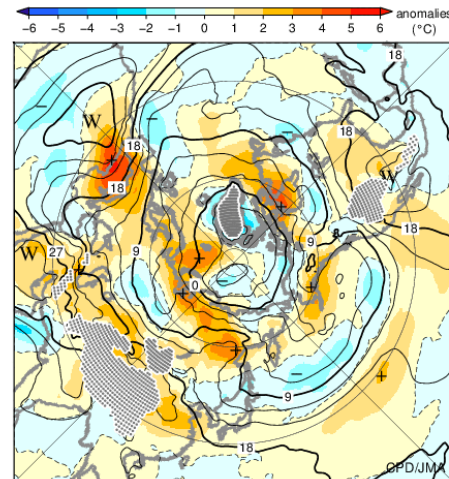
Monthly mean 500 hPa height and anomaly in the Northern Hemisphere (Jun.2022)  
The contours show height at intervals of 60 m.  
The shading indicates height anomalies.  
Anomalies are deviations from the 1991–2020 average.

## SLP anom.



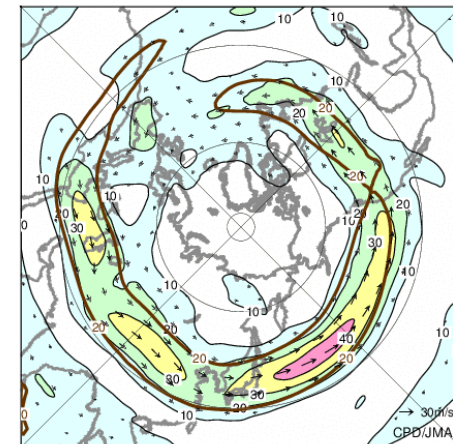
Monthly mean sea level pressure and anomaly in the Northern Hemisphere (Jun.2022)  
The contours show sea level pressure at intervals of 4 hPa.  
The shading indicates sea level pressure anomalies.  
Anomalies are deviations from the 1991–2020 average.

## T850 anom.



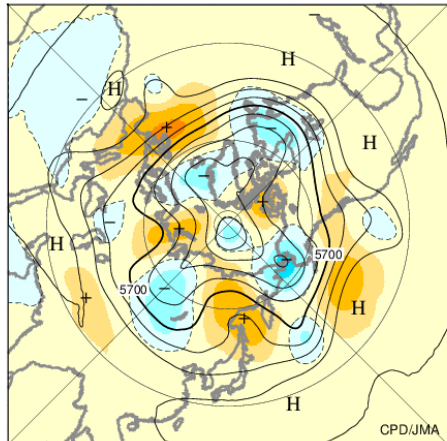
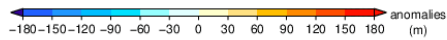
Monthly mean 850 hPa temperature and anomaly in the Northern Hemisphere (Jun.2022)  
The contours show temperature at intervals of 3°C.  
The shading indicates temperature anomalies.  
The hatch patterns indicate areas with altitudes exceeding 1,600 m.  
Anomalies are deviations from the 1991–2020 average.

## U200



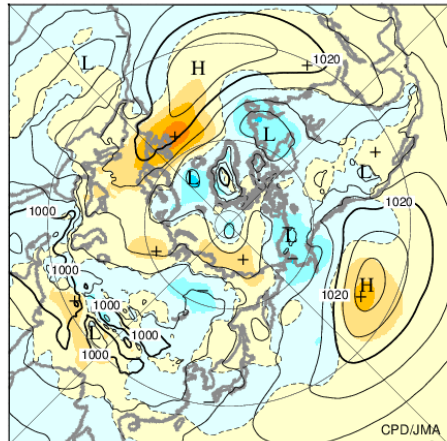
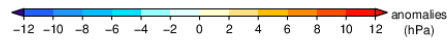
Monthly mean 200 hPa wind speed and vectors in the Northern Hemisphere (Jun.2022)  
The black lines show wind speed at intervals of 10 m/s and the brown lines show its normal (i.e., the 1991–2020 average) at intervals of 20 m/s.  
The vectors are not shown where wind speed is less than 10 m/s.

## z500 anom.



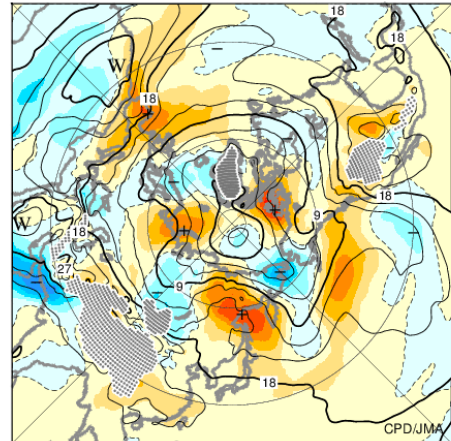
**Monthly mean 500 hPa height and anomaly in the Northern Hemisphere (Jul.2022)**  
The contours show height at intervals of 60 m.  
The shading indicates height anomalies.  
Anomalies are deviations from the 1991–2020 average.

## SLP anom.



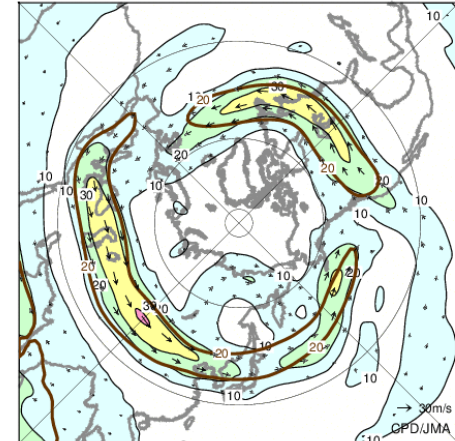
**Monthly mean sea level pressure and anomaly in the Northern Hemisphere (Jul.2022)**  
The contours show sea level pressure at intervals of 4 hPa.  
The shading indicates sea level pressure anomalies.  
Anomalies are deviations from the 1991–2020 average.

## T850 anom.



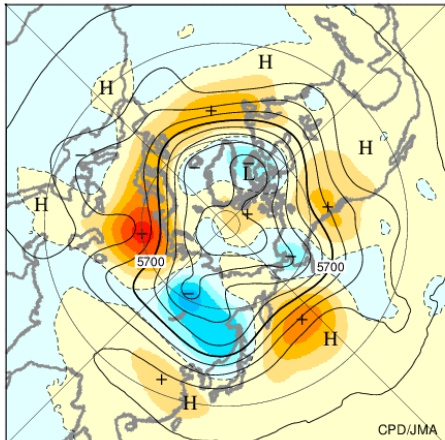
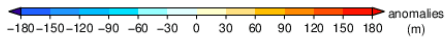
**Monthly mean 850 hPa temperature and anomaly in the Northern Hemisphere (Jul.2022)**  
The contours show temperature at intervals of 3°C.  
The shading indicates temperature anomalies.  
The hatch patterns indicate areas with altitudes exceeding 1,600 m.  
Anomalies are deviations from the 1991–2020 average.

## U200



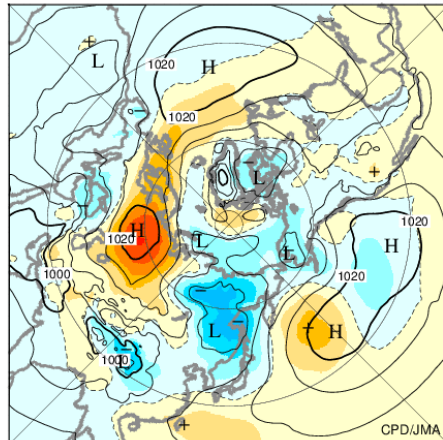
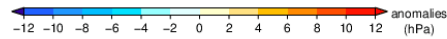
**Monthly mean 200 hPa wind speed and vectors in the Northern Hemisphere (Jul.2022)**  
The black lines show wind speed at intervals of 10 m/s and the brown lines show its normal (i.e., the 1991–2020 average) at intervals of 20 m/s.  
The vectors are not shown where wind speed is less than 10 m/s.

## z500 anom.



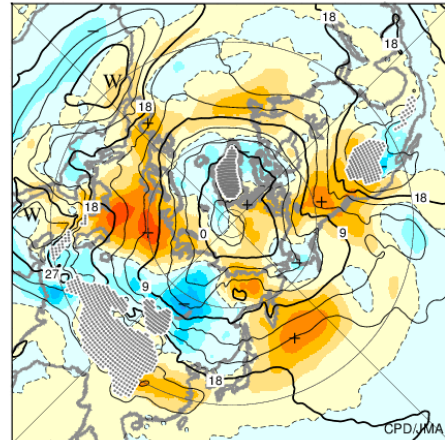
Monthly mean 500 hPa height and anomaly in the Northern Hemisphere (Aug.2022)  
The contours show height at intervals of 60 m.  
The shading indicates height anomalies.  
Anomalies are deviations from the 1991–2020 average.

## SLP anom.



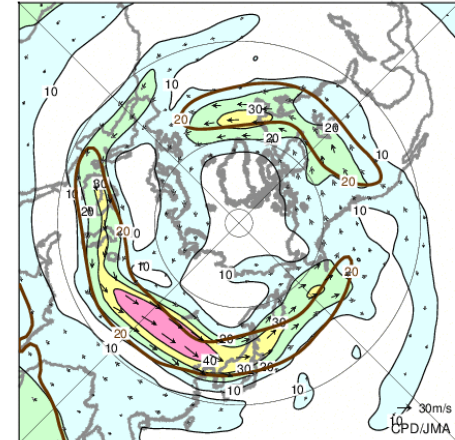
Monthly mean sea level pressure and anomaly in the Northern Hemisphere (Aug.2022)  
The contours show sea level pressure at intervals of 4 hPa.  
The shading indicates sea level pressure anomalies.  
Anomalies are deviations from the 1991–2020 average.

## T850 anom.



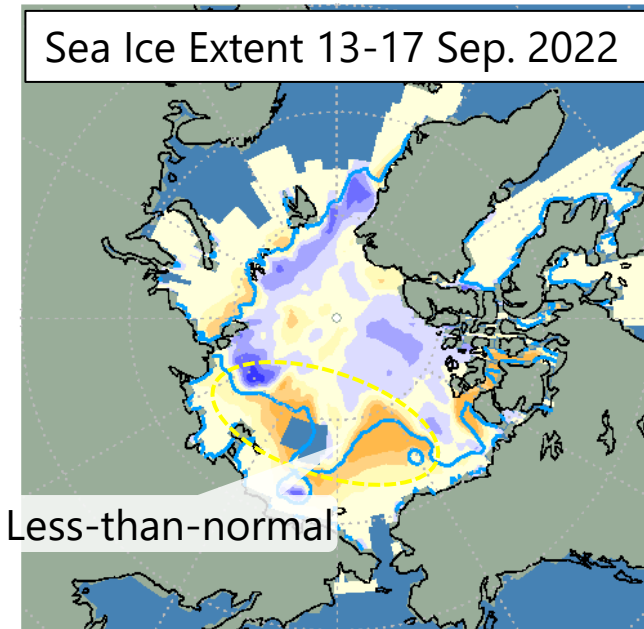
Monthly mean 850 hPa temperature and anomaly in the Northern Hemisphere (Aug.2022)  
The contours show temperature at intervals of 3°C.  
The shading indicates temperature anomalies.  
The hatch patterns indicate areas with altitudes exceeding 1,600 m.  
Anomalies are deviations from the 1991–2020 average.

## U200



Monthly mean 200 hPa wind speed and vectors in the Northern Hemisphere (Aug.2022)  
The black lines show wind speed at intervals of 10 m/s and the brown lines show its normal (i.e., the 1991–2020 average) at intervals of 20 m/s.  
The vectors are not shown where wind speed is less than 10 m/s.

- Arctic sea Ice: Less-than-normal extent in the northern-Eurasian marginal seas
  - [Less arctic-sea ice](#) - [Cold Eurasian winter](#) ?
  - cf. "Warm Arctic and Cold Eurasia" (WACE) pattern (Mori et al.,2014)



Source NSIDC/NOAA <https://nsidc.org/arcticseaicenews/>

Dec.-Feb. T850 regressed on Jun.-Aug. sea ice extent in the northern-Eurasian marginal seas (red closed area)

